

**Principal Component Gradiometer technique for removal of
spacecraft-generated disturbances from magnetic field data
– Response to the Reviewers –**

We thank the Referees for helping us improve the manuscript, which we revised according to their suggestions. In addition, we revised section 2.1 to correct the expression of the matrix \mathcal{G}^{ij} entering the quadrupole correction, which we mistakenly took to be equal to the rotation matrix which transforms the versor $\hat{\mathbf{r}}^j$ to the versor $\hat{\mathbf{r}}^i$. The correct expression is: $\mathcal{G}^{ji} = \mathcal{Q}\mathcal{R}^{ij}\mathcal{Q}^{-1}$ with \mathcal{R}^{ij} being the rotation matrix and $\mathcal{Q}(t)$ the quadrupole moment. This change has no implication on our treatment if only the magnitude of the quadrupolar disturbance changes with time. This was anyway needed by our proposed cleaning method. We explained this in the manuscript (last paragraph of section 2.1).

Below is our response to the Referees comments. It closely follows the Author Comments submitted in the Public Discussion. The Referee comments are typeset in italics, our answers are marked with the \bullet symbol, and the descriptions of the changes made to the manuscript are marked with the \star symbol. A version of the revised manuscript with tracked changes has been also provided.

Referee #1 comments

This material is fully worth publishing as a working record of the cleaning of SOMAG magnetic field data. As an academic paper to discuss the technique which contributes to the better scientific results, I think, the authors have to revise it, at first, to distinguish the matter particular to the SOMAG case from the general matter.

Major comments :

1) The descriptions in section 2 should be considered, because they would be inadequate to explain the basics of the method proposed by the authors. The authors start with expressing the disturbances as the productions of dipole and quadrupole magnetic moments. However, the disturbance characteristic which makes the method described in section 3 applicable is the linear independence at two sensor positions, and therefore disturbances are not necessary to be expressed by the magnetic moments. Although the magnetic moment model would be very useful to optimize the sensor positions and estimate the error, as author did in section 5 and Ness (1971) did, it is not essential to describe the principle of the method proposed by the authors.

\bullet In section 2.1 we demonstrate that for single dipole/quadrupole disturbance sources the problem of deriving the magnetic field produced by a disturber at one location using only the magnetic field measured at another location, has a solution and the solution is unique (equations (2),(3) and (5),(6) on page 3 of the original manuscript ([OM]) / equations (2),(3) and (6),(7) on page 3-4 of the revised manuscript ([RM])). This allows expressing the disturbance magnetic field as a linear combination with time independent coefficients of the difference between the measurements (equation (7) on page 4[OM]/

eq.4 p.4[RM], valid for both dipole and quadrupole disturbances). This in turn is the justification for equation (10) in section 3 (see lines 146-148[OM]/166-168[RM]) on which the proposed cleaning algorithm is based. We believe that this justification is essential for the proposed method and therefore the dipole/quadrupole description of the disturbing sources is necessary.

... the disturbance characteristic which makes the method described in section 3 applicable is the linear independence at two sensor positions ...

- On the contrary, equations (2) and (5)[OM]/(2),(6)[RM] show that the disturbing magnetic field at one position is a linear combination of the components of the disturbing magnetic field at another position, therefore they are not linearly independent. The most general needed characteristic for gradiometer-based methods is equation (7)[OM]/(4)[RM], i.e. the linear relation between the contribution of the disturbance at one point in space and the difference between the measurements taken at that point and those taken at another point. In the particular case of our proposed PiCoG method, an additional necessary property is the linear polarization (i.e. one dimensional character) of the disturbance.

★ If the reviewer actually meant “dependence” (typo error) then we fully agree. We added a few sentences clarifying this at the end of section 2.1 (line 96[OM]/101-102[RM])

2) Descriptions about general rule and requirements are mixed with those about specific conditions to SOMAG and authors assumptions. It makes the readers confuse what is universal to all magnetic field measurement with what is specific to authors case.

- We agree that the text can be misleading. We have to distinguish between two types of disturbance sources. The first one (the one we mentioned in the text) is caused by time variable currents. The field signature caused by this type of disturbance is identical at any measurement position and direction. Only the sign and amplitude depend on position and direction. One can rotate the field measured by a three axes sensor in a (principal axes) coordinate system in which the disturbance is present in one component only. This scalar type of disturbance needs 1 degree of freedom of a sensor difference signal for correction.

In contrast, a rotating magnet (at a sufficient large distance assumed as a rotating dipole) will produce a signature in two directions in a coordinate system aligned to the disturbance signal. We are not treating this type of disturbance in the present work.

We did our best to formulate the cleaning algorithm in its most general form. For single disturbance sources the most general approach is the gradiometer approach, expressed by equation (7)[OM]/(4)[RM]. However, for the algorithm to work when multiple disturbers are present, there are several conditions to be met, which reduce the generality. One important condition required by the PiCoG technique is that the disturbances to be cleaned should vary only in magnitude and should keep their direction constant. From the points (2.1), (2.2), (2.3) raised below, we conclude that by “specific conditions to SOMAG and authors assumptions” the Reviewer refers specifically to this constant di-

rection requirement. This condition is essential for the proposed algorithm. We state in the first paragraph of section 2.2 (lines 98-101[OM]/117-120[RM]) that the universal case of multiple arbitrary disturbers cannot be treated by the proposed algorithm. Next, on page 5 lines 121-122[OM]/141-142[RM] we clearly state that “The PiCoG cleaning method assumes this type of linearly polarized disturbances”. The next sentence allowing for “non-linearly polarized disturbances” is indeed an oversight on our part, confusing for the reader.

★ We added several sentences explaining that the proposed cleaning method only deals with disturbances for which only the module (and not the direction) of the magnetic field changes (after line 49[OM]/54-57[RM]).

★ We removed “or non-linearly polarized disturbances” from line 122[OM].

2-1) page 2 line 47, In many cases the direction of ... I do not think it is often the case.

★ We changed the text after line 47[OM]/51-54[RM] to specify that we refer to disturbances which are large compared to the ambient field during the interval used for cleaning.

2-2) page 5 line 117, but does not change its direction I do not think it is often the case.

• It is explained on lines 120-122[OM]/140-142[RM] that we refer to the disturbances due to time variable currents

2-3) page 6, line 157, For many spacecraft, including GK2A, artificial disturbances keep their direction fixed ... I do not think it is often the case.

★ We changed the text starting with line 157[OM]/186-189[RM] to make it clear that we refer to disturbances due to time variable currents.

3) Many of equations in this paper are derived without enough explanation, and some of them seem to be incorrect.

• Please see the answers (3.2) to (3.7)

3-1) page 3 lines from 70 to equation (8), this part is not understandable due to the shortage of the explanations.

• Please see the answers (3.2), (3.3) and (3.4)

3-2) page 3 line 73, what are k and l ?

• As stated in lines 73-74[OM]/82-83[RM], subscripts stand for components, superscripts stand for positions. k and l are the indices for the Cartesian components. \hat{r}_k is the component k of the unit vector \hat{r} .

★ We explained the meaning of the subscripts and of the superscripts more clearly in the text (lines 74[OM]/83[RM] and 77[OM]/86[RM]).

3-3) page 3 line 79. The inverse ... Please explain the process to derive it. If $(3X-I)^{-1}$

1) = (3/2 X-I), as authors say, (3X-I)(3/2X-I) = I. The left is 9/2 X^2 - 9/2 X + I, so it leads X^2 = X. Is it correct ?

- We do indeed make use of the fact that \mathcal{X} is an idempotent matrix, $\mathcal{X}^2 = \mathcal{X}$. On components, using the Einstein notation (summation over repeating indices):

$$(\mathcal{X}^2)_{ij} = X_{ik}X_{kj} = \hat{r}_i\hat{r}_k\hat{r}_k\hat{r}_j = \hat{r}_i|\hat{\mathbf{r}}|^2\hat{r}_j = \hat{r}_i\hat{r}_j = X_{ij} \quad (1)$$

Now we find a and b such as $(3\mathcal{X} - \mathcal{I})(a\mathcal{X} + b\mathcal{I}) = \mathcal{I}$

$$\Rightarrow (2a + 3b)\mathcal{X} - (1 + b)\mathcal{I} = 0 \quad \forall \mathcal{X} \quad \Rightarrow \quad \begin{array}{l} a = 3/2 \\ \text{and} \\ b = -1 \end{array}$$

Using the idempotency of \mathcal{X} it is easy to check that indeed $(3\mathcal{X} - \mathcal{I})(3\mathcal{X}/2 - \mathcal{I}) = \mathcal{I}$

★ For the sake of readability, we do not include these details in the manuscript.

3-4) page 4 line 84, and $(5X-2I)^{-1}$ is equal to $(5/6X-1/2I)$ if so, again, $X^2 = X$. Is it correct ?

- The inverse of $(5\mathcal{X} - 2\mathcal{I})$ is derived using a similar approach as detailed in (3.3). As proved above, $\mathcal{X}^2 = \mathcal{X}$.

3-5) page 7, line 196, To eliminate the disturbance ... this sentence is difficult to understand. Please make it easy to understand.

★ We change the formulation in the manuscript from

“To eliminate the disturbance b_x^j , the factor in front of it must vanish, therefore”
to

“Since the corrected magnetic field should be independent on the disturbing magnetic field b_x^j , results that the factors multiplying b_x^j in Eqs. (18) must be zero, therefore”

3-6) page 17, equations (29a)(29b)(29c), Please explain how these equations are derived

- To derive the expressions for the matrices \mathcal{M} in Eq. (28) we start by writing the third order correction of the AMR-corrected outboard sensor measurements ($\mathbf{B}^{1,sa}$) using the AMR-corrected inboard sensor measurements ($\mathbf{B}^{1,ta}$) as given by Eq. (26) ($i = s, j = t$):

$$\mathbf{B}^{c,s} = \mathbf{B}^{1,sa} + \mathcal{C}^s(\mathbf{B}^{1,sa} - \mathbf{B}^{1,ta})$$

with \mathcal{C}^s given by Eq. (30) being the factor in front of $\Delta\mathbf{B}^{0,ij}$ in Eq. (26). We then replace the first order AMR corrected inboard and outboard measurements $\mathbf{B}^{1,sa}$ and $\mathbf{B}^{1,ta}$ in the expression of $\mathbf{B}^{c,s}$ above using Eqs. (27) and after some algebra we arrive at

$$\mathbf{B}^{c,s} = \mathcal{M}^s\mathbf{B}^{0,s} + \mathcal{M}^t\mathbf{B}^{0,t} + \mathcal{M}^a\mathbf{B}^{0,a}$$

with $\mathcal{M}^s, \mathcal{M}^t, \mathcal{M}^a$ given by Eqs. (29). Because the DC part of the disturbances is also removed, this form of $\mathbf{B}^{c,s}$ does include implicitly the DC offset \mathbf{G}^s introduced by the correction.

★ We included a brief explanation on how to derive equations (29) after line 382[OM]/431-432[RM].

3-7) page 17, lines 388-399, It is not clear what \hat{G} 's expresses (it cannot be the absolute offset), and how equation (31) is derived.

- Eq. (31) is the definition of \mathbf{G}^s . As the temporal average is taken over the entire time interval used to determine the correction matrices \mathcal{M} , \mathbf{G}^s represents the difference between the mean values before correction and the mean values after the correction, i.e. a constant offset between the original measurements of the outboard sensor, $\mathbf{B}^{0,s}$, and the corrected field. To reduce the correction to a purely AC correction we must subtract this offset from the corrected field, hence the correction which does not introduce a DC offset (defined as the difference between the mean values before and after the correction) is given by Eq. (28). We will revise the formulation in the manuscript to avoid the confusion between the corrected measurements which include the DC offset change due to the AC correction and $\mathbf{B}^{c,s}$ in Eq. (28) for which the DC offset change due to the AC correction is eliminated.

★ We explained more clearly how the DC offset is changed by the proposed procedure and what the \mathbf{G}^s vector represents. This involved changing equation (28) and adding the expression of the pure AC correction. The changes to the text were mostly after the line 389[OM]/439-445[RM].

4) page 3 line 66, Because higher multipole moment ... Here authors say that they can ignore the contribution by higher degree moments. However, later they discuss under the assumption that one of the sensor pair is very closely located to the disturbance source, and therefore the contribution by higher degree moments cannot be negligible. Please make the descriptions consistent.

- While in theory one could place a sensor so close to a disturber such that the octopole (or higher) contribution becomes significant, it is difficult to imagine a real life scenario where the dipole and quadrupole contributions of the disturber do not vastly overwhelm the octopole (or higher) contribution. We are indeed assuming in section 3.1 lines 151-153[OM]/175-176[RM] that the distance from one sensor to the disturber being currently cleaned is small *relative* to the distance to the other disturbers. This does not imply a distance small enough to make octopole and higher orders visible. It merely means that the disturbers are not equally distanced from the sensor in question and one disturber contribution dominates the others.

★ On page 4 lines 107-110[OM]/126-127[RM] we state that the dipole and quadrupole contributions should not have comparable strengths at the sensor location. We changed this sentence to clarify that also higher multipoles should be weak compared with the dominant dipole or quadrupole being cleaned.

★ We clarified that even if we assume a small distance between one of the disturbance sources and one of the sensors, this does not mean that the higher order multipoles become significant (line 152[OM]/176-179[RM]).

5) The proposed strategy to remove the noise argued in this paper seems to be inconsistent. In page 6, line 151, We now assume that one of the terms in Eq. (9) is much larger than the others. ... In page 10 line 2, the placement of the AMRs close to the disturbances sources. To do it, the authors should know the positions of the disturbance sources to locate the sensors nearby. It is inconsistent with the advantage of this method, allows the separation of disturbances generated by the spacecraft ... without prior knowledge about the positions of the disturbances sources. (page 5, line 134) Please make it consistent.

- The observation is correct, of course some knowledge about the disturbers positions is necessary. For instance if a disturber is placed at equal distances from two sensors, the proposed procedure using those two sensors cannot work. It is also assumed that the boom-tip placed sensor is further away from disturbers than the other sensors, and that when the body-mounted sensors accommodations were decided at least some minimum information about the locations of major disturbers was available so sensors could be placed in their vicinity. However, apart from that, the positions of the disturbers do not enter in any way in the cleaning procedure, hence the statement on lines 134-135[OM]/156-168[RM].

★ We changed “positions” to “exact positions” on line 135[OM]/157[RM] and explained at the beginning of section 3.1 (after line 152[OM]/179-181[RM]) that even though the position of the disturbance sources does not enter the PiCoG formalism, some rough information on their location can help optimizing the sensor accommodation.

6) page 9, line 232, 3-axis Flux Gate Magnetometer (FGM)... Is the outboard sensor built based on the design by Primdahl (1979) and inboard one is based on Acuña (2002) ? If not, please refer the papers more adequately.

- Both sensors are neither designed similar to the sensors described in the early Acuña nor in the Primdahl papers. The references are for the fluxgate principle only. The Mario Acuña design consists of three single component sensors accommodated next to each other. The disadvantage of this approach is that the axes directions are determined by the ringcores and the pickup windings and thus they are not stabilised by the more robust feedback coils. In low field conditions (e.g. for the Voyager spacecraft) this is of no importance, however for e.g. MAGSAT it causes a significant uncertainty. Fritz Primdahl has therefore developed a vector compensated magnetometer in which a sensor similar to the sensors developed by Acuña has been placed in a sophisticated feedback coil system compensating the field for all three single sensors in all directions. Xavier Lalanne developed a very nice sensor in which 6 ringcores are placed on the sides of a cube inside a Helmholtz coil system. This is a great design because it is fully symmetric, however very elaborated. Our design is based on two crossed ringcores in the centre of a Helmholtz system. It is described in detail in the Themis Magnetometer paper by

Auster et al.

★ We replaced the references to the Acuña and Primdahl papers with a reference to Auster et al. paper (line 232[OM]/275[RM]).

7) page 10, lines 263-268, I suppose that the sensing alignment relationship between the FGM and AMR sensors would significantly affect the result of the removal of the magnetic disturbances. Please describe the knowledge about the alignment relationship and its accuracy.

• Actually the alignment between the FGM and AMR sensors plays no role in the PiCoG method. This is because the cleaning is performed only on the maximum variance components of the measurements which are independent on alignment.

8) As for the March 4 case presented in this paper, magnetic disturbances are caused by multiple sources and they can be discriminated because the repetition periods are very different one another. The authors should discuss the condition regarding the repetition periods of the disturbances when the proposed method works well and when it does not.

• That is correct. The proposed method works well when the polarization direction of the targeted disturbance is determined by the maximum variance direction. If the disturbances are in the same frequency range and therefore cannot be decoupled by using different window lengths one must either find their polarization direction using other means, or they must have magnitudes different enough such that the dominant disturbance – being currently cleaned – determines the maximum variance direction.

★ We included a new paragraph after line 361[OM]/406-410[RM] which discusses the importance of the characteristic time scale of the disturbances.

9) The order of Figure 2 and Figure 3 should be changed since Figure 3 appears earlier in the text.

• This is correct.

★ We changed the order of the figures 2 and 3

10) The meaning of the word orthogonality in this paper is not clear. If it means linear independence, up to three independent, mutually orthogonal, simultaneously active disturbances can be separated using two sensors. (page 5, line 118) would not be correct. More than three disturbances may be separated if they are linearly independent. The statement in page 14, lines 323-332 should be revised.

• In the manuscript, the word “orthogonal” has the common geometrical meaning: Two directions are called orthogonal if they form a right angle. We say that two disturbances are orthogonal if their maximum variance directions are orthogonal to each other. We will explain this better in the manuscript.

★ We made it clear that we mean orthogonality between the maximum variance directions (lines 118,123,322[OM]/138,141-142,366[RM]).

11) Page 17, section 4.3, What is the advantage to remove the disturbances by the onboard processor ? Because it cannot be guaranteed that the coefficients do not change for long period, it would be much better to determine the coefficients from the raw data on the ground.

- The coefficients were determined from raw data on the ground. Monitoring the magnetic field at geostationary orbit supplies important information about the space weather events reaching the Earth. On-board data cleaning provides near real-time accurate magnetic field data which is essential in this context. An added benefit is a four fold increase in the time resolution achieved by changing the telemetry from raw data from four sensors at one vector per second to cleaned data at four vectors per second.

★ we mentioned this in the Abstract and after line 55[OM]/65[RM]

Referee #2 comments

... The presented method needs the disturbing sources to change with time (variance analysis). In spacecraft magnetical cleanliness DC magnetic disturbers play a big role. On the other hand the offset drift of fluxgate magnetometer is a known problem. Is the method valid for DC calibration? Otherwise write AC disturbance in line 5 (Abstract) and in line 496 (Summary and Conclusion). ...

- If the mean field produced by a disturber is different from zero, i.e. there is a non-zero DC disturbance due to the targeted disturber – which is most of the times the case, the proposed method will automatically correct this DC disturbance if it depends in the same way on the distance to the source as the cleaned AC term (dipole/quadrupole). The total DC shift introduced by the final correction is contained in the \mathbf{G}^s vector given by equation (31). However, even if the above condition is true, the method presented here does not provide the DC offset produced by completely time independent disturbers, therefore it cannot be used for the DC correction. Moreover, the internal offset drift of the sensors cannot be treated using the PiCoG technique.

- ★ We changed the lines in the Abstract and in the Conclusions according to the Referent's request. We also added one sentence stating that the proposed technique deals only with AC disturbances at the beginning of section 2 (line 66[OM]/76-77[RM]).

- ★ We revised the discussion in section 4.3 on the DC contribution introduced by the PiCoG correction.

... The authors call their method to deal with the SOSMAG data PiCoG algorithm. It is more of a methodology than an algorithm that could be coded as is.

- That is correct. We abused the word “algorithm”.

- ★ We replaced “algorithm” with “technique/method” throughout the manuscript.

In chapter 2.1 interesting formulas are deduced for dipole and quadruple fields. They are used to show, that the magnetic field of a low frequency source can be factorized in a time-dependant and a geometry part. But is not that clear anyway for quasi DC magnetic sources?

- Indeed, equations (1) and (4)[OM]/(1),(5)[RM], which are just the expressions for the magnetic field produced by a dipole/quadrupole show the trivial fact that in this case the space dependence can be separated by the time dependence as a factor. The key relations here are equations (2) and (5)[OM]/(2),(6)[RM] which show that the magnetic field produced by a time-dependent dipole/quadrupole at a given location can be obtained using a *time independent* transformation of the magnetic field measured at a different location. This proves that it is in principle possible to use the measurements from one sensor to correct the measurements delivered by another sensor at different location. This is the foundation of our approach.

Do the formulas for the geometry factors enter the evaluation?

- No, the \mathcal{T} matrices given by equations (3) and (6)[OM]/(3),(7)[RM] are not used as such by the PiCoG technique. They might be used perhaps in a very controlled environment when the positions of the sensors and disturbers, as well as the dependence on the distance to the source (dipole/quadrupole) of the disturber are precisely known. This work's goal is to provide a technique which does not require this information. However, the correction matrix \mathcal{A} is related to the \mathcal{T} matrix by the relation in line 146[OM]/170[RM]. This means that – once the \mathcal{A} matrix is computed using the PiCoG method – one could derive the corresponding \mathcal{T} matrix. This is beyond the scope of the present work.

In chapter 3.1. it is assumed, that one of the magnetometers is very close to a disturber. Does the method also work, if that is not the case?

- This depends on the specific sensors-disturbers configuration. E.g. if more disturbers of the same type occupy a volume which is small compared to the distance to the closest sensor, the method works even if the sensor is not closer to one of the disturbers than to the others. If the directions of maximum variance of two disturbers are orthogonal to each other and the disturbances have different time scales, again the method works even if the strength of the two disturbances are the same / disturbers placed at similar distances to the sensor. There are however situations in which the method does not work, as detailed in section 5.

★ We added a paragraph in section 5 after line 425[OM]/479-485[RM] which discusses the case of disturbances of similar strengths at one sensor location.

Unfortunately none of modern methods for analysis of multivariate time series is used. Principal component analysis is one of them. It uses spectral analysis of the cross-covariance matrix of all additional measured magnetometer components with respect to the reference magnetometer. ...

- We *do* use Principal Component Analysis (PCA) as a key method employed by PiCoG. We state this e.g. in lines 119-120, 164-166, 496-497[OM]/139-140, 202-203, 556-557[RM]. It is however not necessary to use all the measured magnetometer components at once as input for the PCA. In our case the PCA reduces to the determination of the variance principal system for the three components of the magnetic field. We indeed determine the direction of maximum variance from the eigenvectors of the covariance matrix as described e.g. in section 1.4 of *Time Series Data Analyses in Space Physics*, Song and Russell, SSR (1999) or in *Analysis methods for multi-spacecraft data*, Sonnerup and Scheible, ISSI Sci. Rep. SR-001, p185-220, Ed Paschmann and Daly, (1998). We do not perform a spectral analysis though because it was not necessary for our specific problem. Of course, if one knows – or determines – in advance that the disturbance to be removed is confined in a specific frequency band, one may perform the PCA in the frequency domain and select the eigenvectors corresponding to the frequency band of the disturbance.

★ We added the above two references to the text (line 165[OM]/194[RM]) and we men-

tioned the possibility to use band pass filtering after line 425[OM]/481[RM].

... The results of sec. 2.1, that means the known geometry factors, add information not been used in standard methods. Using for example the geometry factors for better identifying disturbing time series in the data, or for better determining the distribution of disturbing signal to the different magnetometers would render this paper interesting to a broader public.

- It is true that in this work we did not directly exploit equations (3) and (6)[OM]/(3),(7)[RM] which give the exact expression of the “propagator” matrix \mathcal{T} which allows computing the disturbance at one point in space once the disturbance at another point is known. This would allow cleaning the disturbances using a precise model representing the disturbance sources and the sensors positions. However, this is not the goal of the present work. Here we determine the correction matrices \mathcal{A} – which are equivalent with the \mathcal{T} matrices – solely from the available measurements. Of course, it might be possible to develop an entirely different method using the \mathcal{T} matrices computed based on the precise positions of the disturbers and of the sensors. However, making more intensive use of the \mathcal{T} matrices is not necessary in the context of the present work.

★ We mentioned the possibility of exploiting equations (3) and (6) after line 133[OM]/154-156[RM].

The time dependence of the disturbing signal is not at all used in chapter 3, where the PiCoG Algorithm is defined.

- The time dependence is implicitly used through the fact that the correction is applied to the principal variance component. Also the scaling factor α defined in section 3.1, equation (14) is determined using the variance of the measurements, therefore using the time dependence of the disturbing signal.

... Nevertheless during the actual data evaluation the authors implicitly use the time dependence by looking at different time periods, with different sources active. Fig. 2 shows the distribution of directions on a sliding window. Later on, in chapter 4. ramps and spikes are used to validate the result. These tricks should be included in the PiCoG algorithm.

- We made efforts to keep the PiCoG method described in section 3 as general as possible (please see also Referent #1 comment 2). Including procedures specific to our particular application of the method to the SOSMAG data would in our opinion induce confusion to the reader. Presenting these procedures in the application section on the other hand, lets the reader decide for him/herself if these procedures are appropriate or not for his/her problem at hand. Even for our specific problem we did not used the same procedures from the beginning to the end: For the AMR correction we determined the maximum variance direction using just one step-like disturbance, while for the FGM-FGM correction we decided for a statistical approach using a sliding window.

The variance of measured date is used. That means field sources (ambient and disturbing

fields) are understood as random processes. The motivation is not clear.

- It is true that variance normally refers to the the deviation of a random variable from its mean value. A certain randomness is introduced by the ambient field. However, in the context of the present work, the random/non-random character of the disturbance plays no role. We use the variance only as a measure of how strong the AC disturbance is in each direction, and through PCA we determine the direction in which the variance is largest therefore the disturbance is strongest.

★ We explained better how the variance analysis is used by PiCoG and clarified that for our purposes it is not necessary for the disturbance or for the ambient field to be generated by a random process (after line 164[OM]/196-197[RM]).

...The step amplitudes in all components could directly be used to deduce the geometry factors (Component of Matrix A in formula 10) between different magnetometers.

- The correction matrix \mathcal{A} is composed from a rotation and a scaling. We don't see a direct way to deduce the \mathcal{A} matrix from step amplitudes. After the rotation in the VPS one could indeed determine the amplitude of the steps as we did in section 5 and from them derive the scaling factor α in equation (13a). We think however that equation (14) gives a more general solution. Both estimates of the α factor are susceptible to improvements anyway as mentioned in lines 273-274[OM]/316-318[RM].

Fig. 4. Shows magnetometer values in the coordinate system orientated along the main axes of the data variances ellipsoid (VPS system). The figure shows, that the spike signal is still present in the z- and in the y-direction. Accordingly the VPS x-direction does not point along the spike disturbance.

- This is correct. The x -axis of the VPS in Figure 4 is aligned with the variance direction of the highest frequency disturbance (first to be cleaned), distinct from the direction of the spikes. This is discussed on lines 321-324[OM]/365-368[RM]. The VPS in which the data in Figure 5 is represented has its x -axis aligned with the direction of the spikes.

L39: The PiCoG Process also is not running on the SC.

- The PiCoG technique delivers the correction matrices \mathcal{M} which are uploaded to the spacecraft and used for onboard data cleaning. As far as we understand, the *Poppe et al. (2011)* procedure cannot be reduced to a simple linear combination which can easily be implemented onboard.

L48: This is the case if only variances are looked at. But the authors look later at ramps and spikes. They can even be identified, if they point along the ambient field.

- We use the PCA/variance analysis also for the ramps and for the spikes. This is specified in multiple places in section 4.2. One could use other methods to determine the direction of the ramps or spikes disturbances (even manually perhaps), but the PCA delivers the correct directions and the scale factors in an automatic fashion.

★ We emphasize in the text the use of PCA for the MD disturber: line 269[OM]/312[RM]

L48: The term principal component is misleading. It usually refers to direction of a main axe of the stray ellipse in a multivariate random process.

- The term “principal component” in the text does indeed refer to the main axis of the variance ellipsoid. The fact that the disturbance is not a random process does not affect neither the application of the PCA nor its results.

★ We mentioned on line 165[OM]/196-197[RM] that we do variance analysis without implying random processes.

L107: Perhaps better: a collection of dipoles will in general generate multipole moments

- The suggested formulation is indeed better. Thank you.

★ We changed the text according to the Referent’s suggestion.

L 151: Which term is much larger? Would a strong disturber really make only one term large?

- Since the summation index q in equation (9) refers to the disturbance sources – as detailed in line 137[OM]/160[RM], the term corresponding to the strong/close disturber will be larger. A strong disturber will only affect the corresponding term in the sum.

L137 this sentence would be more readable, if the summation symbol was omitted.

★ We re-phrased this sentence to make it more readable.

L157: Do you mean: disturbing magnetic moments are fixed in direction with moments changing with time?

- Yes, this is what we mean.

★ We adapted the text.

L158: The stray field of one disturber has a constant direction in the magnetometer system. No need for a new coordinate system.

- The stray field of one disturber has indeed a constant direction in the magnetometer system. However, a new coordinate system is needed to align this direction with one of the coordinate system axes (in our case the x -axis).

L166: Using this VPS suggests, that the disturber itself is a multivariate random process. But that is not the case. The VPS- x direction can be calculated by correlating the disturbing field strength with the measured x -, y -, z - components. The term variance principle system is misleading. The reader could get the impression, that principal component analysis was done.

- PCA was in fact done in order to obtain the disturbance direction. As stated before, the non-random character of the disturbing field is not relevant in this context. One could probably obtain the disturbance direction by minimizing the correlation between the disturbing field strength and the measured y and z components using as free parameters

the angles of rotation for the new system. We do not see the advantage in using this alternative method.

★ We mentioned on line 165[OM]/196-197[RM] that we perform variance analysis without implying random processes.

L167: Are the alpha i,j in Eq. 13a the same as the $A_{i,j}$ in Eq. 10? Than please use the same denomination.

- They are not the same. \mathcal{A}^{ij} in equation (10) is the matrix used to correct sensor i measurements using sensor j measurements. $\alpha^{0,ij}$ in equation (13) is a scalar scaling factor given by equation (14) for the first order correction.

L191: It is not clear to me if the b s are known at this point and if yes, where they are calculated.

- The disturbance b at the sensor position is not known at this point. We only make use of the dependence on the distance of b as stated in lines 193-195[OM]/235-237[RM].

L211: Do you mean if stray fields of different disturbers are not coincident at the magnetometer location?

- We mean “if stray fields of different disturbers do not share the same direction at the magnetometer location”.

★ We have revised the text.

I quit following the text here because the authors use a matrix notation, where I guess vectors of stray fields are sufficient.

- We do not see how to concisely write the relations without using matrix notation.

Conclusion: The paper is an excellent report on how the authors achieved to clean and calibrate SOSMAG data. However the term principal component technique in the title is misleading. The authors should revise the method and try to use or at least refer to standard methods for multivariate data analysis and, if possible, expand them to produce a paper of more general interest.

- We thank the Reviewer for the appreciative comment. However, as explained above on several occasions, PiCoG *is* using principal component analysis as a essential tool, therefore we believe the title is appropriate. We changed the title nevertheless, please see our answer to the Reviewer’s reaction bellow.

★ We change the title to “Maximum Variance Gradiometer technique for removal of spacecraft-generated disturbances from magnetic field data”.

Referee #2 reaction to response

“PiCoG algorithm” : *Would you think that the following procedure is in line with what you did. Could this be a line out of an algorithm?*

1. Define one of the N instruments as “reference instrument”.
 2. Calculate the differences of all instruments and the reference instrument.
 3. In all difference signals, identify the instrument j showing the strongest disturbance.
 4. Use this difference to correct all instrument readings using Eg. 13
 5. For the next iteration start over with 2. disregarding instrument j .
- No, we use a different procedure:

Assume three magnetometers, m_0 , m_1 and m_2 and two disturbance sources, d_1 and d_2 . Assume we define instrument m_0 as reference instrument. Assume the dominant disturbance at the instrument m_1 location comes from the source d_1 and the dominant disturbance at the instrument m_2 location comes from the source d_2 .

Assume the difference is largest for the instrument m_1 , i.e. $|\text{var}(\Delta \mathbf{B}^{01})| > |\text{var}(\Delta \mathbf{B}^{02})|$. In these conditions equations (13) will work correctly to clean the disturbance d_1 from the measurements taken by the reference instrument m_0 and – if desired – also from the measurements taken by the instrument m_1 .

However, as explained in lines 170-173[OM]/207-209[RM], beside the $(\Delta \mathbf{B})_x$ term, which is written in the VPS of the difference $\Delta \mathbf{B}$, all other terms in equations (13) are written in the VPS of the measurements at the respective instruments. The maximum variance x -axis computed for the instrument m_2 will be aligned with the direction of the disturbance d_2 at the location of the instrument m_2 which in general will be different from the direction of the disturbance d_1 at the location of the instrument m_2 . Therefore equations (13) used as suggested by point 4 above, would apply the correction for the disturbance d_1 to the wrong component of the measurements taken by the instrument m_2 . Moreover, the scaling factor computed using the variance of the measurements from the instrument m_2 will also be wrong.

In contrast, the PiCoG technique uses one instrument pair at a time: After points 1-3 above, we clean the (strongest) disturbance d_1 from the measurements of the reference instrument m_0 . Afterwards we compute the difference between the cleaned measurements from the reference instrument m_0 and the measurements from the instrument m_2 . This difference will now reflect the disturbance d_2 . We determine the VPS of the difference and of the measurements from the instrument m_2 and we finally apply again equations (13) to clean the disturbance d_2 from the cleaned measurements taken by the reference instrument m_0 .

Note that the method works without knowledge about the exact positions of the sources and – after the correction matrices are determined on ground – it works with simple multiplications and additions, which can be done in real time by the onboard software.

PCA: You determine the main axes in the 3D distribution of magnetometer measurements and in the distribution of differences between two different magnetometers. Then you assume that your α can be calculated based on the quotient of variances along these

main axes (Eq. 14). This is a very bold assumption and you named quite some requirement for this assumption.

- Up to a constant factor, the difference $\Delta \mathbf{B}$ is the same as the disturbance at the sensor to be cleaned (same time dependence). The factor is the ratio between the amplitude of the difference and the amplitude of the disturbance at the sensor to be cleaned. This can be directly derived from the variances. As mentioned on line 174[OM]/215-216[RM], equation (14) gives a first order estimation of the scaling factor α . This estimation may deviate from the exact scaling factor due to large ambient field fluctuations or due to additional disturbances with the same polarization direction as the disturbance to be cleaned. To improve this value one may for instance minimize the correlation between the corrected measurements and the disturbance represented by the difference $\Delta \mathbf{B}$ as we note on lines 271-274[OM]/315-318[RM]. However, in our case this proved not to be necessary.

★ We explain this better after line 173[OM]/213-216[RM].

Asking for PCA, I meant to use PCA in the 3N dimensions of all available measured time series. If PCA is referred to in the title the reader will expect it to be used on the multivariate time series

$(X_1(t), Y_1(t), Z_1(t), \Delta X_{21}(t), \Delta Y_{21}(t), \Delta Z_{21}(t), \Delta X_{31}(t), \Delta Y_{31}(t), \Delta Z_{31}(t), \dots)$.

“1” being the reference magnetometer. This automatically produces what you call VPS-x directions (as components of the largest eigenvector).

- PCA done in 3 dimensions is not something unusual in space physics data analysis, see e.g. section 1.4 “Principal Axis Analysis” of *Time Series Data Analyses in Space Physics*, Song and Russell, SSR (1999). There might be a way to use PCA in 3N dimensions for cleaning multi-sensor data, but the exact implementation of this is not obvious to us. The maximum eigenvalue and the corresponding eigenvector derived for the multivariate time series suggested by the Reviewer would somehow mix the reference instrument measurements with the differences between those measurements and the measurements from all other instruments. Moreover, as explained above, if different disturbances affect different sensors, they will also be mixed together, even if initially they were decoupled from one another. This is exactly what we are trying to avoid. Even if perhaps possible, at the moment we do not see how a technique based on PCA in 3N dimensions can be implemented for cleaning multi-sensor data. As we showed by applying it to SOSMAG data, the (3D PCA) procedure proposed by us works well to decouple and clean spacecraft disturbances, and, in our opinion, is general enough to be easily adapted to other multi-sensor configurations.

★ We explained after line 159[OM]/194-196[RM] that we determine the principal components using only the 3D time series from individual sensors.

... Please judge for yourself whether the reference to PCA in the title is really justified.

- We realise that some readers might expect a treatment along the lines suggested by the Reviewer, therefore we change the title to “Maximum Variance Gradiometer technique

for removal of spacecraft-generated disturbances from magnetic field data”.

But even PCA and factor analysis do not deliver unique results. In PCA geometry factors are completely ignored. Therefore exploitation of Eq. 3 and Eq. 6 would introduce a completely new idea going further than what can be done by PCA.

- Using the equations (3) and (6) would be indeed a very different approach from the one presented by us. It is definitely worth exploring ways to use these relations to develop new methods – perhaps model-based – for cleaning multi-sensor data. Once developed, such methods could be combined with the PiCoG technique to improve the results, but this should be the focus of another study.

On page 6 between line 157 and line 180 you argue very intuitively. This lack of mathematical rigor should be mitigated using PCA in the way I proposed.

- As explained above, a direct application of PCA in $3N$ dimensions is not a solution for our problem. On page 6 we write down the expressions of the corrected measurements under the stated assumptions. We do not see where the lack of mathematical rigour lies.

It is absolutely not clear how Eq. 10 follows from Eq. 9. I even doubt, that a linear relation between the correction value for B^i and the $\Delta B^{i,j}$ exists. This is only true if only one single disturber is on. I guess Eq.10 is the first order approach assuming that a certain disturber is very prominent (at a certain time span) in the difference $\Delta B^{i,j}$. Please clarify and explain that in the text.

- Equation (10) does indeed not follow equation (9) in the general multiple disturber case. We will reformulate the text to better explain that equation (10) is valid for single disturber case.

★ We changed the text after line 143[OM]/166-168[RM] to better explain that equation (10) is valid for single disturber case.

~~Principal Component~~ Maximum Variance Gradiometer technique for removal of spacecraft-generated disturbances from magnetic field data

Ovidiu Dragoş Constantinescu^{1,2}, Hans-Ulrich Auster¹, Magda Delva³, Olaf Hillenmaier⁴, Werner Magnes³, and Ferdinand Plaschke³

¹Institute for Geophysics and Extraterrestrial Physics, TU Braunschweig, Germany

²Institute for Space Sciences, Bucharest, Romania

³Space Research Institute, Austrian Academy of Sciences, Graz, Austria

⁴Magson GmbH, Berlin, Germany

Correspondence: D. Constantinescu (d.constantinescu@tu-bs.de)

Abstract.

In situ measurement of the magnetic field using space borne instruments requires either a magnetically clean platform and/or a very long boom for accommodating magnetometer sensors at a large distance from the spacecraft body. This significantly drives up the costs and the time required to build a spacecraft. Here we present an alternative sensor configuration and ~~an~~ algorithm allowing for ulterior a technique allowing for removal of the spacecraft generated AC disturbances from the magnetic field measurements, thus lessening the need for a magnetic cleanliness program and allowing for shorter boom length. The ~~proposed algorithm~~ final expression of the corrected data takes the form of a linear combination of the measurements from all sensors, allowing for simple onboard software implementation. The proposed technique is applied to the Service Oriented Spacecraft Magnetometer (SOSMAG) onboard the Korean geostationary satellite GeoKompsat-2A (GK2A) ~~which uses for the~~ first time a. In contrast to other missions where multi-sensor ~~configuration for onboard data cleaning~~ measurements were used to clean the data on ground, the SOSMAG instrument performs the cleaning onboard and transmits the corrected data in real time, as needed by space weather applications. The successful elimination of the AC disturbances originating from several sources validates the proposed cleaning technique.

1 Introduction

15 Since very early in space exploration it has become clear that the main limitation in performing accurate magnetic field measurements came not from the instruments themselves but rather from the strong artificial magnetic fields generated by the spacecraft carrying them. It was recognized that there are three possible approaches to mitigate this problem: One could limit the electromagnetic emissions coming from the spacecraft by going through a rigorous magnetic cleaning procedure. This is a costly and complicated engineering task and introduces limitations on building and operating other onboard instruments, see
20 e.g. (Narvaez, 2004) for details on the magnetic cleanliness program for Cassini magnetic field experiment (Dougherty et al., 2004). Another approach is to accommodate the magnetometer at a large distance from the spacecraft, usually at the end of a

long boom, such as the 12 m long Kaguya boom (Kato et al., 2010) or the 13 m long Voyager boom (Behannon et al., 1977). This introduces constraints on the spacecraft operations and still requires a certain degree of magnetic cleanliness of the spacecraft in order to keep the boom at reasonable length. A third way is to accept the presence of spacecraft generated disturbances in the measured magnetic field and to remove the artificial contributions afterwards onboard or on ground through special techniques (Mehlem, 1978; Georgescu et al., 2008; Pope et al., 2011). An extreme case, where no magnetic cleanliness and no boom was provided is e.g. the magnetic field experiment on the MASCOT lander (Herčík et al., 2017). In most cases however, a combination of two or all of the approaches above is employed. For instance, Cluster (Escoubet et al., 1997) and THEMIS (Angelopoulos, 2008) are magnetically clean spacecraft carrying magnetometers on relatively long booms. For normal science investigations, the stray magnetic field from these spacecraft is well below the required accuracy and no further steps to remove it are usually necessary. Venus Express (Titov et al., 2006) on the other hand, was a magnetically dirty spacecraft with two magnetometers (Zhang et al., 2006) mounted on a short boom for which extensive data cleaning efforts had to be undertaken (Pope et al., 2011). A comprehensive overview of the instrumentation and challenges related to measuring magnetic fields in space is given by Balogh (2010). In this work we focus on the third approach: removal of the contribution of the spacecraft generated magnetic field from the measured data, without the need of extensive information on potential spacecraft disturbance sources.

One of the first studies on using multi sensor measurements to clean magnetic field data measured onboard spacecraft, came from Ness et al. (1971). The proposed method was then successfully applied in a simplified manner to Mariner 10 magnetic field data (Ness et al., 1974) assuming one single dipole disturber source. Neubauer (1975) gave a detailed error analysis of the Ness et al. (1971) method and discussed the optimum placement of collinear sensors. The more recent cleaning procedure used by Pope et al. (2011) for Venus Express, though based on the same principle, is much more sophisticated allowing removal of disturbances from several different sources. However, additional information about the spacecraft operation and fuzzy logic had to be used to distinguish between the disturbance sources. Such a complex algorithm would be difficult to implement for onboard data cleaning. Our aim is a correction method which reduces to a linear (or at most quadratic) combination of the magnetic field values measured by several sensors without input from other sources, therefore easy to implement onboard.

Similarly with Ness et al. (1971) and Pope et al. (2011) methods, the disturbance removal method described in the following sections is based on the fact that the magnetic field measured by each sensor is the sum of the ambient magnetic field and the artificial magnetic field generated by the spacecraft. Because the ambient field is the same for all sensors, it vanishes in the difference between the measurements from any two sensors, similar with the gradiometer working principle. The difference is entirely determined by the artificial magnetic field sources from the spacecraft, preserving their time dependence. Magnetic disturbances generated by time-dependent currents flowing through simple mechanically fixed current loops keep constant direction, therefore in general the disturbance affects only one component of the measured field. ~~In many cases the~~ If the variation of the disturbing magnetic field is much larger than the variation of the ambient magnetic field during the time interval selected to determine the cleaning parameters, the direction of the strongest disturbance ~~coincides~~ will coincide with the principal component (maximum variance component) of the measured field, allowing application of the correction only to the affected component. This is the type of magnetic disturbances which can be treated using the method described in the

next sections. If the direction of the disturbance changes in time – as it is the case for instance for magnetic fields produced by flywheels or other moving mechanisms – then another approach must be used.

The proposed method is applied to the SOSMAG instrument (Auster et al., 2016; Magnes et al., 2020) which, together with the Particle Detector experiment (Seon et al., 2020) is part of the Korea Space wEather Monitor (KSEM) (Oh et al., 2018) onboard the GeoKompsat-2A (GK2A) geostationary spacecraft. SOSMAG consists of four three-axial magnetic field sensors, two of them mounted on a short boom extended from the spacecraft, the other two placed near strong magnetic disturbance sources within the spacecraft. Once the correction coefficients are determined on ground, they are uploaded to the spacecraft and are used by the onboard software to correct in-flight the magnetic field measurements. This enables accurate magnetic field measurements ~~onboard GK2A~~ which are delivered in near real-time to the ground stations without the need of passing through a magnetic cleanliness program before launch. The quick data delivery is essential in the context of space weather monitoring.

The remaining of the paper is organized as follows: In sec. 2 we discuss the gradiometer principle on which our method is based. Sec. 3 outlines the proposed Principal Component Gradiometer (PiCoG) method to remove spacecraft generated disturbances from the measured magnetic field data. Sec. 4 describes how the PiCoG method is applied to clean the GK2A SOSMAG data. The limitations of the proposed method are discussed in sec. 5. Sec. 6 summarises our work.

2 Disturbances from known sources

This section gives the analytical expressions for disturbances when the exact locations of the magnetic field sources and of the sensors are known. While in most cases the direct application of these expressions is not practical, the section outlines the general principle used by gradiometer-based disturbance cleaning methods, namely the possibility to express the spacecraft generated disturbances in terms of differences between measurements taken at distinct places. The relations derived here constitute the basis of the PiCoG ~~algorithm~~ technique detailed in section 3. They are valid for both AC and DC disturbances, though the PiCoG technique only deals with AC disturbances. Because higher multipole moments attenuate strongly with the distance to the source and become negligible even for short booms, we will concentrate only on the dipole and quadrupole contributions.

2.1 Single disturbance source

The magnetic field produced at the position $\mathbf{r} = r\hat{\mathbf{r}}$ by a dipole characterised by a slowly varying time dependent magnetic moment $\mathbf{M}(t)$ is given by:

$$\mathbf{b}(\mathbf{r}, t) = \frac{\mu_0}{4\pi r^3} (3\mathcal{X}(\hat{\mathbf{r}}) - \mathcal{I}) \mathbf{M}(t) \quad (1)$$

where the elements $X_{kl} = \hat{r}_k \hat{r}_l$ of the matrix \mathcal{X} are given by the product between the components of the position versor $\hat{\mathbf{r}}$, and \mathcal{I} is the 3×3 identity matrix. The subscripts k and l refer to Cartesian components. Knowing the magnetic field at the position \mathbf{r}^i , one can compute the magnetic field at any position \mathbf{r}^j without knowledge about the source magnetic moment $\mathbf{M}(t)$:

$$\mathbf{b}(\mathbf{r}^j, t) = \mathcal{T}^{\text{dip}}(\mathbf{r}^i, \mathbf{r}^j) \mathbf{b}(\mathbf{r}^i, t) \quad (2)$$

where the superscripts i and j denote the measurement positions and the time-independent linear transformation \mathcal{T}^{dip} is:

$$\mathcal{T}^{\text{dip}}(\mathbf{r}^i, \mathbf{r}^j) = \left(\frac{\mathbf{r}^i}{\mathbf{r}^j} \right)^3 (3\mathcal{X}^j - \mathcal{I})(3\mathcal{X}^i - \mathcal{I})^{-1} \quad (3)$$

90 The inverse $(3\mathcal{X} - \mathcal{I})^{-1}$ always exists and is equal to $(3/2\mathcal{X} - \mathcal{I})$.

~~Similar relations can be written for a time-dependent quadrupole defined by its moment $\mathcal{Q}(t)$:~~

$$\underline{\mathbf{b}(\mathbf{r}, t)} = \underline{\frac{\mu_0}{4\pi r^4} (5\mathcal{X}(\hat{\mathbf{r}}) - 2\mathcal{I}) \mathcal{Q}(t) \hat{\mathbf{r}}}$$

$$\underline{\mathbf{b}(\mathbf{r}^j, t)} = \underline{\mathcal{T}^{\text{quad}}(\mathbf{r}^i, \mathbf{r}^j) \mathbf{b}(\mathbf{r}^i, t)}$$

$$\underline{\mathcal{T}^{\text{quad}}(\mathbf{r}^i, \mathbf{r}^j)} = \underline{\left(\frac{\mathbf{r}^i}{\mathbf{r}^j} \right)^4 (5\mathcal{X}^j - 2\mathcal{I}) \mathcal{G}^{ji} (5\mathcal{X}^i - 2\mathcal{I})^{-1}}$$

95 ~~where \mathcal{G}^{ji} is the rotation matrix which transforms the versor $\hat{\mathbf{r}}^j$ to the versor $\hat{\mathbf{r}}^i$ and $(5\mathcal{X} - 2\mathcal{I})^{-1}$ is equal to $(5/6\mathcal{X} - 1/2\mathcal{I})$. To derive the above relations~~ To derive this we used the fact that ~~\mathcal{Q} is a symmetric matrix, $\mathcal{Q}^T = \mathcal{Q}$ and \mathcal{X} is an idempotent matrix, $\mathcal{X}^2 = \mathcal{X}$.~~

Assuming that the ambient magnetic field is generated by distant sources and thus it is the same at the positions \mathbf{r}^i and \mathbf{r}^j , it is possible to separate the contribution $\mathbf{b}(\mathbf{r}^i, t)$ ~~from due to~~ a nearby dipole ~~or quadrupole~~ from the ambient field by computing
100 the difference between the measured magnetic field at the two positions:

$$\mathbf{b}(\mathbf{r}^i, t) = (\mathcal{T}^{\text{dip}}(\mathbf{r}^i, \mathbf{r}^j) - \mathcal{I})^{-1} (\mathbf{B}_{\text{measured}}(\mathbf{r}^j, t) - \mathbf{B}_{\text{measured}}(\mathbf{r}^i, t)) \quad (4)$$

where the total measured magnetic field $\mathbf{B}_{\text{measured}}(\mathbf{r}, t) = \mathbf{B}(t) + \mathbf{b}(\mathbf{r}, t)$ contains both the position-independent ambient magnetic field $\mathbf{B}(t)$ and the position-dependent disturbance magnetic field $\mathbf{b}(\mathbf{r}, t)$. Sensor specific disturbances such as sensor noise and sensor offset will be considered later.

105 Note that the ~~\mathcal{F} matrices only depend~~ \mathcal{T}^{dip} matrix only depends on the position vectors \mathbf{r}^i and \mathbf{r}^j . ~~They are~~ It is independent on the dipole $\mathcal{M}(t)$ ~~or quadrupole $\mathcal{Q}(t)$ moments and perform and performs~~ a similar function with the propagator operator in quantum mechanics. Equation (4) shows that once the ~~\mathcal{F}~~ \mathcal{T}^{dip} matrix is determined for a pair of sensors, measurements from those two points are sufficient to separate the contribution from a single magnetic field source with arbitrary time variation from the ambient magnetic field. This is the theoretical justification for our method. Also note that for Eq. (4) to be satisfied it
110 is not strictly necessary that the disturbance has a dipole character. It is enough that a (time independent) linear relation exists between the disturbing magnetic field affecting the sensors at the positions \mathbf{r}^i and \mathbf{r}^j

Similar relations can be written for a time-dependent quadrupole defined by its moment $\mathcal{Q}(t)$:

$$\underline{\mathbf{b}(\mathbf{r}, t)} = \underline{\frac{\mu_0}{4\pi r^4} (5\mathcal{X}(\hat{\mathbf{r}}) - 2\mathcal{I}) \mathcal{Q}(t) \hat{\mathbf{r}}} \quad (5)$$

$$\underline{\mathbf{b}(\mathbf{r}^j, t)} = \underline{\mathcal{T}^{\text{quad}}(\mathbf{r}^i, \mathbf{r}^j) \mathbf{b}(\mathbf{r}^i, t)} \quad (6)$$

$$115 \quad \underline{\mathcal{T}^{\text{quad}}(\mathbf{r}^i, \mathbf{r}^j)} = \underline{\left(\frac{\mathbf{r}^i}{\mathbf{r}^j} \right)^4 (5\mathcal{X}^j - 2\mathcal{I}) \mathcal{G}^{ji} (5\mathcal{X}^i - 2\mathcal{I})^{-1}} \quad (7)$$

where $G^{ji} = Q R^{ij} Q^{-1}$. R^{ij} is the rotation matrix which transforms the versor \hat{r}^i to the versor \hat{r}^j and $(5\mathcal{X} - 2\mathcal{I})^{-1}$ is equal to $(5/6\mathcal{X} - 1/2\mathcal{I})$. While there are instances when $\mathcal{T}^{\text{quad}}$ is independent on the quadrupole moment $Q(t)$ (e.g. when the quadrupole source and the two sensors are aligned), in general $\mathcal{T}^{\text{quad}}$ depends on it.

For our purposes however, it is important that $\mathcal{T}^{\text{quad}}$ does not depend of time. A common situation when this happens is when only the magnitude of the quadrupolar disturbance depends on time. Then the time dependence can be separated as an independent scalar factor in the expression of the quadrupole moment, $Q(t) = q(t)Q_0$ and therefore $\mathcal{T}^{\text{quad}}$ becomes time independent. A relation similar with Eq. (4) can then be written also for the quadrupole and the disturbance can be removed using the same procedure as for a dipole disturbance. In what follows we assume this kind of time variation for quadrupole sources.

2.2 Multiple disturbance sources

The contributions from more than one simultaneously active, arbitrary placed source with arbitrary time dependence cannot be separated from the ambient field in a simple way. However, if multiple sensors are arranged in a suitable configuration and if specific properties of the disturbers, such as known polarization or time dependence are used, it is possible to remove disturbances generated by multiple sources.

Two magnetometers represent the minimal configuration needed to eliminate stray spacecraft magnetic fields. Many spacecraft carry two magnetometers attached at different positions along one boom. If the boom is long enough such that the distances between the disturbance sources are much smaller compared to the distances to the measurement points and if the disturbances have all either pure dipole or quadrupole character, then their \mathcal{T} matrices will be the same and their collective disturbance can be separated from the ambient field in one step using only two sensors as it was done e.g. by Ness et al. (1974). Of course, any a collection of dipoles will generate in general produce multipole moments. For the procedure to work, the quadrupole contribution and higher order contributions must be much weaker than the dipole contribution at both sensors. If however, both dipole and quadrupole contributions are present at the same time with comparable strengths, then their \mathcal{T} matrices will differ due to the different attenuation with the distance. In this case, one must rely on specific properties of the disturbance to eliminate the quadrupole contribution.

In contrast to the minimum two magnetometer configuration, one can imagine a configuration such as for each disturber there is a sensor placed much closer to it than to all other disturbers, plus an additional sensor far away from all disturbers. Then for each sensor the far disturbers can be assimilated to the ambient field and the problem becomes the single disturber problem discussed at the beginning of the section. Each contribution can then be separated from the ambient field independently. Such a sensor configuration is ideal and can be attained with a number of sensors placed within the spacecraft plus one sensor placed on a short boom.

If the disturbing magnetic field has a time dependent magnitude but does not change its direction, i.e. its variation is linearly polarized, then up to three independent, mutually orthogonal with mutually orthogonal variance directions, simultaneously active disturbances can be separated using two sensors. This is done by projecting Eq. (4) on the direction of each disturbance. The direction of each disturbance can be determined using principal component analysis as described in sections 3 and 4. This

150 kind of linear polarized disturbances produced by fixed configuration time-dependent currents are commonly encountered. The PiCoG cleaning method assumes this type of linearly polarized disturbances. If more than three disturbances, ~~or non-linearly polarized disturbances, or disturbances or disturbances~~ with their polarization directions not mutually orthogonal are present, then information from more sensors is necessary. Different sensor pairs will correct different disturbances.

The SOSMAG configuration on board of the GK2A spacecraft lies somewhere in between the ideal configuration above
 155 and the minimum two magnetometers configuration. It consists of two high accuracy magnetometers placed on a relatively short boom and a number of resource saving magnetometers placed inside the spacecraft. As we will show in section 4, this configuration is well suited to apply the PiCoG cleaning method.

3 The Principal Component Gradiometer ~~algorithm~~technique

The PiCoG cleaning ~~algorithm~~technique is based on the fact that while the ambient magnetic field does not change over the
 160 spacecraft scale, the magnitude of a spacecraft generated disturbance in the magnetic field decreases with the distance to the disturbance source. Therefore, the disturbance can be ~~recovered~~detected – and subsequently removed from the useful signal – by comparing measurements from sensors placed at different distances to the disturbance source as outlined in section 2. ~~Here we describe the derivation of the~~

~~If the precise positions of the disturbers and of the sensors are known, then the~~ transformation matrices \mathcal{T} which ~~allows~~
 165 ~~allow~~ the separation of disturbances generated by the spacecraft ~~can be computed directly. The measurements are then cleaned using Eq. (4) and the equivalent equation for quadrupole disturbers. However, this is in general not the case. Here we describe the derivation of the \mathcal{T} -matrices~~ under certain assumptions ~~, but without prior knowledge about the exact positions of the disturbance sources.~~

The magnetic field measured by the sensor i can be written as the sum of the ambient magnetic field, $B(t)$, the ~~disturbance~~
 170 ~~$\sum_{q=1}^N b^q(t, r^{iq}) = \sum_{q=1}^N b^{qi}(t)$ sum of the disturbances $b^q(t, r^{iq}) = b^{qi}(t)$~~ created by N ~~disturbance~~ sources placed at relative positions $r^{iq} = r^i - r^q$ from the sensor i and a term containing the sensor specific disturbance (noise and time dependent offset), $Z^i(t)$:

$$B^{0,i}(t) = B(t) + \sum_{q=1}^N b^{qi}(t) + Z^i(t) \quad (8)$$

where the index zero ~~on the left side~~ indicates the initially measured magnetic field.

175 We can eliminate the ambient field by subtracting the measurements from two sensors placed at ~~different~~distinct positions:

$$\Delta B^{0,ij}(t) = B^{0,i}(t) - B^{0,j}(t) = \sum_{q=1}^N \Delta b^{qij}(t) + \Delta Z^{ij}(t) \quad (9)$$

~~To remove the disturbance in the measured data we have to find the correct coefficients A_{kl}^{ij} for~~

~~If we neglect the sensor specific disturbances, for single disturbers, the correction to be applied to the measurements consists of~~ a linear combination of the components of the difference $\Delta B^{0,ij}(t)$ between the measured magnetic field at each sensor

180 position:

$$B_{\text{corrected}}^i(t) = B^{0,i}(t) + \mathcal{A}^{ij} \Delta B^{0,ij}(t) \quad (10)$$

If we neglect the sensor specific disturbances, for single disturbers the matrix \mathcal{A}^{ij} is the same as the matrix $(\mathcal{T}(\mathbf{r}^i, \mathbf{r}^j) - \mathcal{I})^{-1}$ in Eq. (4). Using Eq. (4) we find that the matrix \mathcal{A}^{ij} is equal to $-(\mathcal{T}(\mathbf{r}^i, \mathbf{r}^j) - \mathcal{I})^{-1}$. For each sensor pair i, j a matrix \mathcal{A}^{ij} must be determined. This may of course be computed if we know the exact coordinates of the sensors and of the disturbers and if the disturbers are pure single dipoles or quadrupoles. This is in general not true, therefore we will derive the correction matrix \mathcal{A}^{ij} directly from the measurements.

3.1 First order correction

We now assume that one of the terms in Eq. (9) is much larger than the others. This is true if one of the disturbance sources is much stronger or much closer to one of the sensors than to the others. In this case ~~equations the corrected measurements~~ are given by Eq. (10). Note that the small distance between the disturbance source and a sensor does not imply significant contribution from higher order multipoles. It merely implies that the dominant dipole/quadrupole term produced by the source in question at the sensor location is much larger than the contribution from the other disturbance sources. Also note that even though the positions of the disturbers do not enter the PiCoG formalism, some rough information about the positions of major disturbers can help in optimising the accommodation of the sensors by placing them near major disturbers.

195 Equations (8) and (9) are reduced to the single disturber form are:

$$B^{0,i}(t) = B(t) + \mathbf{b}^i(t) + \mathbf{Z}^i(t) \quad (11)$$

$$\Delta B^{0,ij}(t) = \Delta \mathbf{b}^{ij}(t) + \Delta \mathbf{Z}^{ij}(t) \quad (12)$$

where we drop the disturbance source index, q .

For many spacecraft, including GK2A, ~~artificial disturbances keep their direction fixed at a given sensor position and only their magnitudes vary in time proportional to their (instantaneous) magnetic moment.~~ many artificial disturbances are produced by simple fixed geometry currents without phase delays and thus their magnetic moments are fixed in direction with only their modules changing in time. ($\mathbf{M}(t) = m(t)\mathbf{M}_0$ and/or $\mathbf{Q}(t) = q(t)\mathbf{Q}_0$) Therefore, in the proper coordinate system, only one component of the measured field is affected by one disturbance source. ~~However, since in general the direction of the disturbance varies from sensor to sensor, different reference systems must be used for different sensors~~ This is a key condition for applying the PiCoG technique.

To find the direction of the disturbance at the sensors positions we need to assume that the variance due to the disturbance at the sensor positions determines the maximum variance direction of the measured magnetic field. This holds either when the variance of the disturbance is much larger than the variance of the ambient field or when the variance of the ambient field does not have a preferred direction. In this case, the direction of the disturbance at both sensors can be estimated through variance analysis and the (Sonnerup and Scheible, 1998; Song and Russell, 1999) of the 3D time series from each sensor. The principal components at each sensor are then the magnetic field components along the maximum variance directions. The

variance is used as a measure of how strong the AC disturbance is in each direction. The maximum variance direction identifies the strongest component (the only component in case of linear polarization) of the disturbance both for regular and random disturbances.

215 Our strategy is first to isolate the disturbance as the maximum variance component of the differences $\Delta \mathbf{B}^{0,ij}$, then to use it to correct only the maximum variance component of the measurements $\mathbf{B}^{0,i}$. Since in general the direction of the disturbance varies from sensor to sensor, different reference systems must be used for different sensors and for the measurements differences.

220 The components of the magnetic field at the sensor i , corrected using measurements from the sensor j , can be written in the variance principal system (VPS) of the sensor i measurements as:

$$B_x^{1,ij} = B_x^{0,i} - \alpha^{0,ij} (\Delta \mathbf{B}^{0,ij})_x \quad (13a)$$

$$B_y^{1,ij} = B_y^{0,i} \quad (13b)$$

$$B_z^{1,ij} = B_z^{0,i} \quad (13c)$$

225 The superscript “1” in equations Eqs. (13) stands for the first order correction. Note that while the left hand sides and the first term of the right hand sides of equations Eqs. (13) are represented in the VPS of the measurements at the sensor i , $(\Delta \mathbf{B}^{0,ij})_x$ in the right hand side of Eq. (13a) is represented in the VPS of the difference $\Delta \mathbf{B}^{0,ij}$. The VPS has the x -axis aligned with the maximum variance and the z -axis aligned with the minimum variance. Equation (13a) reflects the fact that the correction for the maximum variance component of the measured magnetic field $\mathbf{B}^{0,i}$ is proportional to the maximum variance component of the difference $\Delta \mathbf{B}^{0,ij}$. The other two components of the measured magnetic field remain unaffected by the correction.

230 A Since the difference $(\Delta \mathbf{B}^{0,ij})_x$ is proportional to the disturbance to be cleaned, the scaling factor $\alpha^{0,ij}$ in Eq. (13a) is the ratio between the amplitude of the difference and the amplitude of the disturbance at the position of the sensor i . Assuming that most of the variance of the magnetic field measured by the sensor i is due to the disturbance to be cleaned, a first estimation of the $\alpha^{0,ij}$ factor is given by the variance of the measurements:

$$\alpha^{0,ij} = \pm \sqrt{\frac{\text{Var}\left((\mathbf{B}^{0,i})_x\right)}{\text{Var}\left((\Delta \mathbf{B}^{0,ij})_x\right)}} \quad (14)$$

235 The \pm sign above is due to the fact that while the orientation of the x axis of the VPS is determined from variance analysis, its sense remains arbitrary. If necessary, the scaling factor value computed using Eq. (14) can be refined e.g. by minimizing the correlation between the corrected magnetic field $B_x^{1,ij}$ and the difference $(\Delta \mathbf{B}^{0,ij})_x$.

240 If $\mathcal{R}^{0,i}$ is the rotation matrix from the sensor system to the VPS of the measurements from the sensor i , and $\mathcal{R}^{0,ij}$ is the rotation matrix from the sensor system to the VPS of the difference $\Delta \mathbf{B}^{0,ij}$, then in the sensor system equations Eqs. (13) take the form:

$$B_k^{1,ij} = B_k^{0,i} - \alpha^{0,ij} \left((\mathcal{R}^{0,i})^{-1} \right)_{kx} \left(\mathcal{R}^{0,ij} \Delta \mathbf{B}^{0,ij} \right)_x \quad ; k = 1, \dots, 3 \quad (15)$$

In matrix form the above relation can be written as:

$$\mathbf{B}^{1,ij} = \mathbf{B}^{0,i} + \mathcal{A}^{0,ij} \Delta \mathbf{B}^{0,ij} \quad (16)$$

where the matrix \mathcal{A} with elements

$$A_{kl}^{0,ij} = -\alpha^{0,ij} \left((\mathcal{R}^{0,i})^{-1} \right)_{kx} \left(\mathcal{R}^{0,ij} \right)_{xl} \quad (17)$$

is the correction matrix for the first (strongest) disturber. Note that there is no implicit summation over repeating indices.

3.1.1 Collinear case

While not required, the special case when the disturbance source is collinear with the two sensors is instructive. In this case, the direction of a linearly polarized disturbance will be the same at both sensors, therefore the same coordinate system will be used for ~~equations Eqs.~~ (13). Substituting $B_x^{0,i}$ in the Eq. (13a) using Eq. (11), we obtain:

$$B_x^{1,ij} = B_x + (a - \alpha^{0,ij}(a - 1))b_x^j + Z_x^i - \alpha^{0,ij}(Z_x^i - Z_x^j) \quad (18a)$$

$$B_x^{1,ji} = B_x + (1 + \alpha^{0,ji}(a - 1))b_x^j + Z_x^j - \alpha^{0,ji}(Z_x^j - Z_x^i) \quad (18b)$$

where we made use of the proportionality between the spacecraft generated disturbances at the sensors i and j : $b_x^i = ab_x^j$. For a dipolar disturber at distance r^i from the sensor i , and r^j from the sensor j , $a = (r^j/r^i)^3$. For a quadrupolar disturber $a = (r^j/r^i)^4$.

~~To eliminate the disturbance~~ Since the corrected magnetic field should be independent on the disturbing magnetic field b_x^j , the factor in front of it must vanish it results that the factors multiplying b_x^j in Eqs. (18) must be zero, therefore

$$\alpha^{0,ij} = \frac{a}{a - 1} \quad \text{and} \quad \alpha^{0,ji} = \frac{-1}{a - 1} \quad (19)$$

This shows that in the collinear case, the sum of the α coefficients is equal to one:

$$\alpha^{0,ij} + \alpha^{0,ji} = 1 \quad (20)$$

A consequence of the above is that the difference between the corrected measurements at the two sensors is always zero:

$$\Delta B_x^{1,ij} = B_x^{1,ij} - B_x^{1,ji} = (1 - \alpha^{0,ij} - \alpha^{0,ji})(b_x^i - b_x^j + Z_x^i - Z_x^j) \equiv 0 \quad (21)$$

In other words, the corrected field is the same regardless which sensor is used as “primary” sensor: $B_x^{1,ij} = B_x^{1,ji}$

For α obeying Eq. (19) the corrected field given by ~~equations Eqs.~~ (18) is:

$$B_x^{1,ij} = B_x + Z_x^i - \alpha^{0,ij}(Z_x^i - Z_x^j) \quad (22)$$

Comparing the above with Eq. (11) shows that, apart from eliminating the spacecraft generated disturbance b_x^i , the procedure introduces an additional disturbance which mixes the two sensor specific disturbances Z_x^i and Z_x^j scaled by $\alpha^{0,ij}$, potentially increasing the noise in the corrected measurements. This effect was also noted by Delva et al. (2002). However, if $\alpha^{0,ij}$ approaches unity (disturbance source much closer to sensor i), the i sensor specific noise is replaced by the j sensor specific noise which might lead to reduced noise.

3.2 Higher order corrections

Further corrections can be iteratively applied as long as the ~~maximum-variance-directions-of-the-disturbances-do-not-coincide-~~
~~stray fields from different disturbers do not have the same direction at the magnetometer location.~~ The iteration relation from
order $n - 1$ to order n is

$$275 \quad B^{n,ij} = B^{n-1,ij} + \mathcal{A}^{n-1,ij} \Delta B^{n-1,ij} \quad ; \quad B^{0,ij} = B^{0,i} \quad (23)$$

with

$$A_{kl}^{n-1,ij} = -\alpha^{n-1,ij} \left((\mathcal{R}^{n-1,i})^{-1} \right)_{kx} \left(\mathcal{R}^{n-1,ij} \right)_{xl} \quad (24)$$

The $\alpha^{n,ij}$ coefficient is estimated from the variance of the field corrected up to order n . The rotation matrices $\mathcal{R}^{n,i}$ and $\mathcal{R}^{n,ij}$ refer to the order n corrected field.

280 Using Eq. (23) and Eq. (24) we find the corrected magnetic field in the second and third order written as linear combinations
of the difference of the measurements taken at the two sensors:

$$B^{2,ij} = B^{0,i} + \left(\mathcal{A}^{0,ij} + \mathcal{A}^{1,ij} + \mathcal{A}^{1,ij} (\mathcal{A}^{0,ij} + \mathcal{A}^{0,ji}) \right) \Delta B^{0,ij} \quad (25)$$

$$\begin{aligned} B^{3,ij} = B^{0,i} + & \left(\mathcal{A}^{0,ij} + \mathcal{A}^{1,ij} + \mathcal{A}^{2,ij} \right. \\ & + \mathcal{A}^{1,ij} (\mathcal{A}^{0,ij} + \mathcal{A}^{0,ji}) + \mathcal{A}^{2,ij} (\mathcal{A}^{0,ij} + \mathcal{A}^{0,ji} + \mathcal{A}^{1,ij} + \mathcal{A}^{1,ji}) \\ & \left. + \mathcal{A}^{2,ij} (\mathcal{A}^{1,ij} + \mathcal{A}^{1,ji}) (\mathcal{A}^{0,ij} + \mathcal{A}^{0,ji}) \right) \Delta B^{0,ij} \end{aligned} \quad (26)$$

285 The corrected field $B^{n,ij}$ determined for the sensor i can replace now the measured field $B^{0,i}$ in a similar procedure
involving the next (third) sensor, until the measurements from all sensors are used.

Ideally, the hardware should consist of a “main”, least disturbed sensor and additional sensors close to each major disturbance
source as described in section 2.2. Then, only the first order correction for each sensor pair containing the main sensor is
necessary to clean the data. However, also other sensor configurations can be used as described in the next section.

290 4 Application to GK2A SOSMAG measurements

The GK2A spacecraft launched on December 4 2018 on a 128.2° East geostationary orbit is operated by the Korea Aerospace
Research Institute (KARI) and provides meteorological and space weather monitoring over the Asia-Pacific region. The mag-
netic field vector is measured by the SOSMAG instrument (Magnes et al., 2020) at four locations onboard the spacecraft:
~~two-~~ Two high accuracy 3-axis Flux Gate Magnetometers (FGM) (~~Primdahl, 1979; Acuña, 2002~~) with a design similar to the
295 THEMIS FGM instruments (Auster et al., 2008) are placed at the end (outboard sensor, FGMO) and respectively 80 cm from
the end (inboard sensor, FGMI) of an approximatively one meter long boom, ~~and two-~~ The other two magnetometers are 3-axis
Anisotropic Magnetic ~~Resonance~~ Resistance (AMR) (Brown et al., 2012) solid state magnetometers placed ~~within-on~~ the body
of the spacecraft.

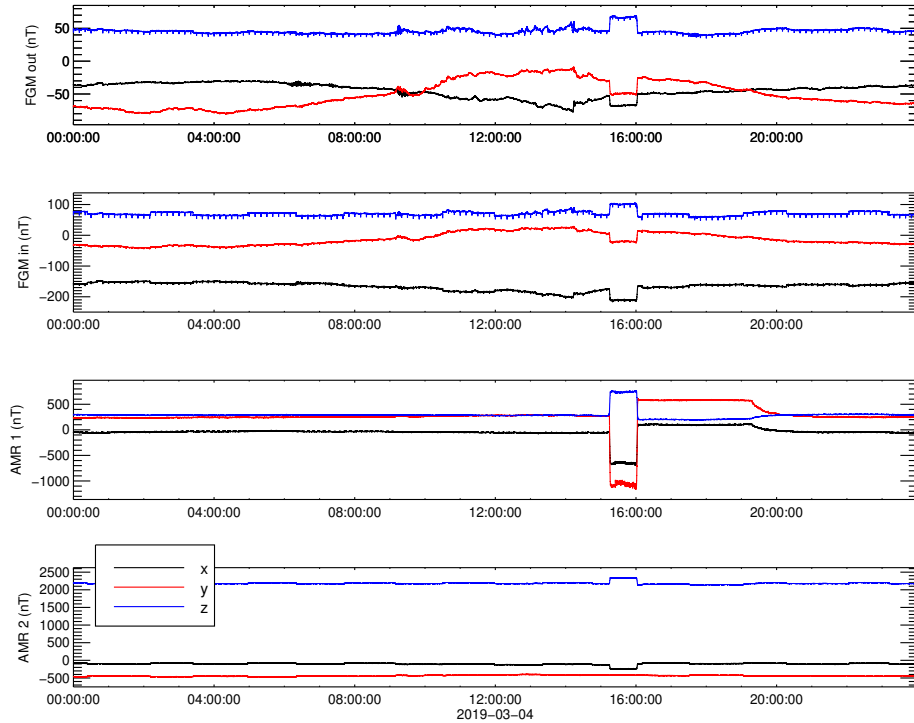


Figure 1. The components in the OB sensor system of the uncorrected measurements taken by the four magnetometers onboard GK2A on March 4 2019. From top to bottom: FGM0, FGMI, AMR1, and AMR2.

The placement of the sensors can be seen in Fig. 6 of Mages et al. (2020). Compared with the spacecraft dimensions, (290 × 240 × 460) cm, the magnetometer boom is relatively short, leading to strong spacecraft-generated disturbances at both FGM sensors.

As far as magnetic cleanliness is concerned, GK2A is a black box, i.e. no access to spacecraft operation time tables and to satellite specific housekeeping data is available to aid the cleaning of the magnetic field data. Therefore the cleaning process must be based exclusively on the magnetic field measurements. Our goal is to eliminate the time dependent spacecraft generated disturbances from the FGM measurements. The strategy we adopt in order to take maximum advantage of the high accuracy of the FGMs and of the placement of the AMRs close to the disturbance sources, is to first use the AMR measurements to clean the data from both FGMs, and then use these corrected measurements to clean each other.

When a disturbance is much stronger at one sensor – as it is the case for the AMR sensors – the scaling factor α is roughly given by the ratio of the magnitudes of the disturbance at the two sensors. This ratio is about 40 for AMR1, and 5 for AMR2, when paired with any of the FGMs. Since the sensor specific noise for the flux gate magnetometers is lower by a factor of 20 compared to the AMR sensor noise, according to Eq. (22), the correction using the AMR sensors will introduce roughly the AMR noise divided by α . In particular, for the AMR2 one fifth of its noise would be introduced in the corrected measurements.

Since the same main disturbance is seen by both AMR sensors, no extra information is present in the AMR2 measurements, therefore we decided not to use the AMR2 sensor for removing the stray time dependent spacecraft magnetic field. The $1/40$ from the AMR1 noise is much more favourable therefore we will use this sensor to clean both FGM sensors measurements.

4.1 FGM outboard and FGM inboard cleaning using the AMR1

Figure 1 shows the uncorrected measurements taken by the outboard FGM, inboard FGM and the two AMR sensors on March 4 2019. We choose this day because it is representative for the routine operations, all the disturbance sources are active and the ambient field shows little variance. Both step-like and spike-like disturbances can easily be seen in the picture. Among them, a prominent step-like disturbance between about 15:00 and 16:00 is clearly detected by all four sensors, showing a very large magnitude at the AMR1. Note that the disturbance, which starts shortly after 15:00 affects the measurements until around 20:00. Because at 15:00 UT the spacecraft is close to local midnight we call this disturbance “midnight disturbance” (MD) to distinguish it from the other step-like disturbances. In 2019 this disturbance appears daily at the beginning and at the end of the year for about 14 weeks in total. We begin the cleaning of the data by first removing this disturbance from the FGM sensors measurements using the AMR1 data.

For the sake of clarity, in the following we use the index s for the outboard FGM, the index t for the inboard FGM, and the index a for the AMR1 sensor. Equation (16) giving the magnetic field measured by the FGM sensors corrected in the first order using the AMR1 sensor yields:

$$\mathbf{B}^{1,sa} = \mathbf{B}^{0,s} + \mathcal{A}^{0,sa} (\mathbf{B}^{0,s} - \mathbf{B}^{0,a}) \quad (27a)$$

$$\mathbf{B}^{1,ta} = \mathbf{B}^{0,t} + \mathcal{A}^{0,ta} (\mathbf{B}^{0,t} - \mathbf{B}^{0,a}) \quad (27b)$$

with the matrices $\mathcal{A}^{0,ja}$; $j = s, t$ given by Eq. (17).

We select the time interval [15:10,16:15] to isolate the targeted disturbance and use it to ~~calculate the~~ determine the variance directions of the disturbance and the scaling factors which give us the correction matrices. To lift the indetermination of the sign of the scaling factor α in Eq. (14) we compute the corrected fields Eq. (27) for both signs and keep the sign for which the disturbance is successfully removed. Equation (14) gives a very good estimation for the scaling factor. However, since this estimation uses the measured magnetic field which includes the ambient magnetic field, it may slightly deviate from the correct value. To improve the precision one may use the scaling factor determined from Eq. (14) as initial value for a minimization procedure of the correlation between $(\Delta \mathbf{B}^{0,ja})_x$ and the corrected $(\mathbf{B}^{1,ja})_x$. While we found this to improve the determination of α for FGMI-FGMO cleaning for days with disturbed ambient magnetic field, for the AMR1 cleaning on March 4 2019, the minimization does not change significantly the value of α .

The angle between the direction of the disturbance at the AMR1 sensor and the direction of the disturbance at the inboard FGM sensor is 31° . For the outboard FGM sensor this angle is 25° indicating that the disturbance source is not collinear with either of the sensor pairs. This is not surprising given the placement on the spacecraft body of the AMR sensors. Even so, the sum of the α coefficients differs from unity with less than 0.005.

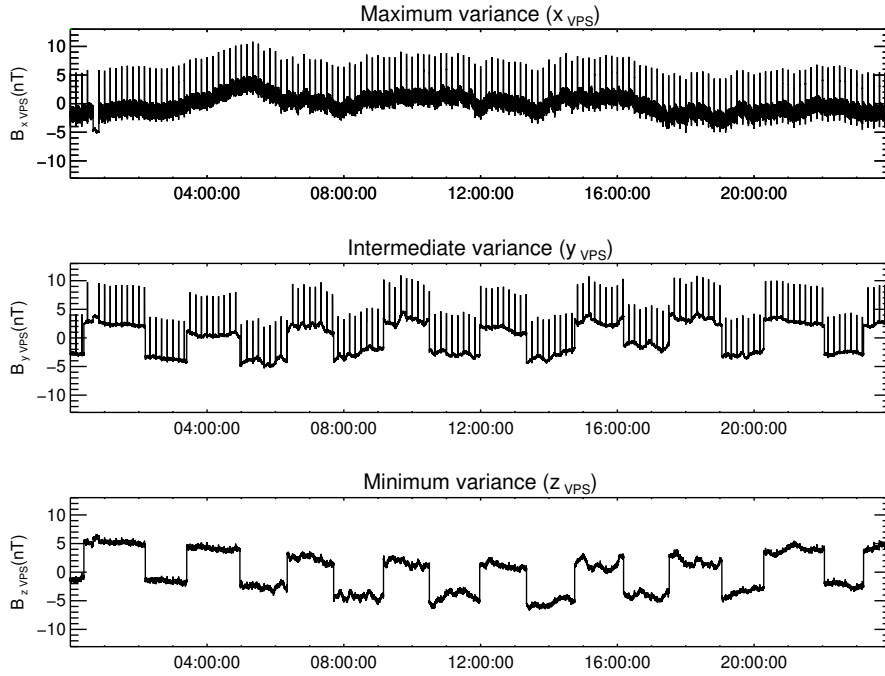


Figure 2. The cleaning parameters resulting from difference ΔB^{st} before the sliding-window scan for the first order correction of was applied, represented on components in its corresponding VPS (the outboard FGM. The left panel shows x -axis is aligned with the number density of the maximum variance variation direction (θ_w, φ_w) on a $1^\circ \times 1^\circ$ grid. The right panel shows a histogram of the statistical distribution of the α_w coefficients ΔB^{st} . The grey filled bars are the coefficients corresponding to directions within 2.5° mean values were subtracted from most probable directional all components. The red vertical line marks their mean value.

345 The higher order corrections should identify and eliminate disturbances roughly ordered by their strength at the AMR1 location. However, attempting the second order correction only introduces spurious data in the FGMs measurements, increasing their variance. This is because the noise level of the AMR sensors is higher than the noise level of the FGM sensors and the AMR1 noise is added to the corrected measurements according to Eq. (22). Consequently we limit the AMR1 corrections to the first order.

350 Since the data cleaning onboard the spacecraft should not require frequent updates of the correction parameters once uploaded to the spacecraft, it is necessary that the determined \mathcal{A} correction matrices remain stable in time. In order to confirm this we checked the stability of the cleaning parameters by using the same procedure once for every week showing the targeted disturbance in 2019. The standard deviation for the maximum variance directions was below 1° , while the standard deviation for the scale factors was below 10^{-3} . These low values are not surprising since for a given source the cleaning parameters
355 depend only on its multipole character and on the geometry of the sources-sensors system. Other factors such as the intensity

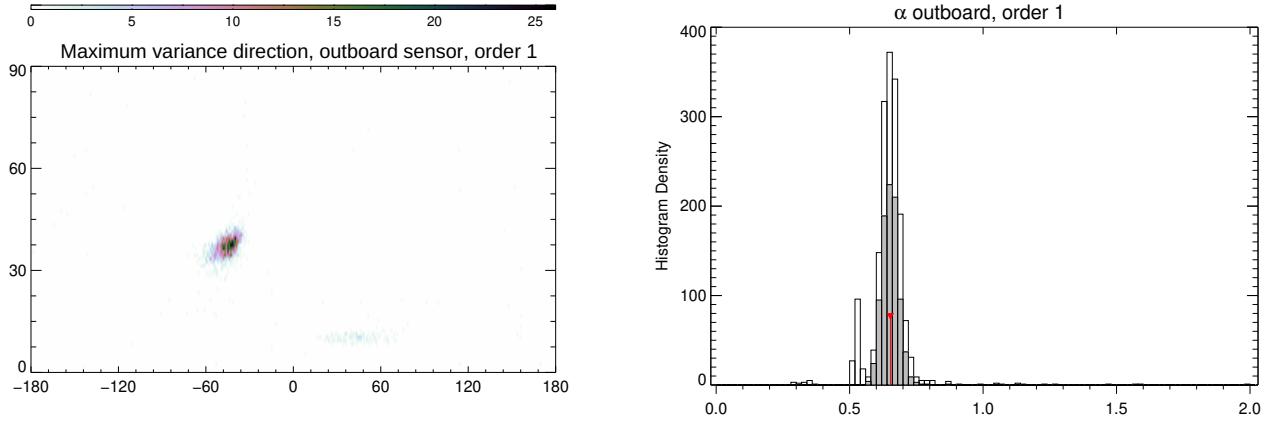


Figure 3. The difference ΔB^{st} represented on components in its own VPS before cleaning parameters resulting from the sliding window scan for the first order correction was applied of the outboard FGM. The mean values were subtracted left panel shows the number density of the maximum variance direction (θ_w, φ_w) on a $1^\circ \times 1^\circ$ grid. The right panel shows a histogram of the statistical distribution of the α_w coefficients. The grey filled bars are the coefficients corresponding to directions within 2.5° from all components most probable direction. The red vertical line marks their mean value.

of the current generating the magnetic disturbance or the temperature do not influence the cleaning parameters. Applying the correction using the determined set of parameters removes the disturbance throughout the entire 2019 year.

4.2 FGM cleaning using the AMR1-corrected data

We now use the AMR1-corrected FGMO and FGMI measurements given by Eq. (27) as starting point in the iteration Eq. (23)
 360 for cleaning the FGMO data using the FGMI data and vice-versa.

Unlike the single step disturbance we dealt with in section 4.1, the disturbances to be removed now show a repetitive pattern over the entire day, apparent in Fig. 1. Apart from the removed large magnitude disturbance, one can visually identify at least two other types of disturbances in Fig. 1: step-like disturbances at a time scale of over one hour, and spike-like disturbances at time scales of minutes. To determine the correct cleaning parameters, the length of the analysis interval has to be chosen such
 365 as to contain many samples of the targeted disturbance but avoid including other disturbances. This can be accomplished by eliminating first the highest frequency disturbances using small enough interval length. Then the interval length is increased to encompass the next frequent disturbance.

In order to increase the precision of the cleaning and to have an indication on the stability of the determined parameters we compute the cleaning parameters using sliding windows covering the entire 24 h interval. For each window w we find the
 370 scaling factor α_w , the elevation angle θ_w and azimuth angle φ_w of the maximum variance direction. After we scan the entire day interval, we determine the most probable direction (θ, φ) of the maximum variance which determines the rotation matrices

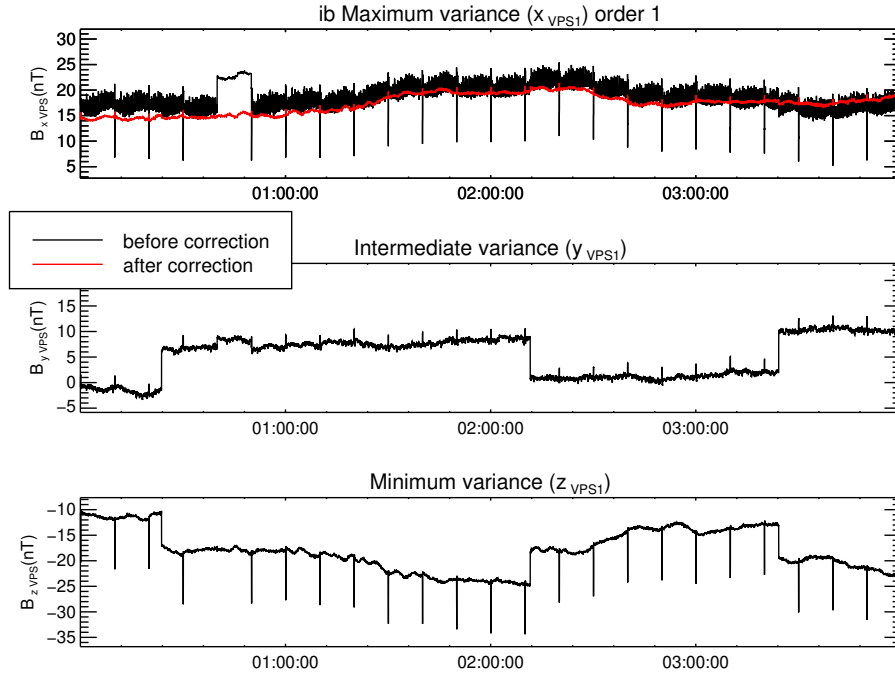


Figure 4. The initial AMR1-corrected FGM inboard measurements represented in the inboard VPS are plotted with the black lines. The first order correction is plotted with red. Mean values were subtracted.

\mathcal{R} in Eq. (24). For this direction we select the corresponding coefficients α_w and we compute their average value. At the end, the correction matrix \mathcal{A} is computed using θ, φ and α .

The disturbances can be much better identified in the difference $\Delta B^{0,sta} = B^{0,sa} - B^{0,ta}$ plotted in Fig. 2. The difference
375 was first rotated in the VPS corresponding to a window length of 100 s, smaller than the time interval between the spike-like disturbances. In this coordinate system, different disturbance types tend to sort themselves on components.

The spike-like disturbances appear now in the x and y components with a cadence of 10 min and an magnitude larger than 10 nT during the entire interval. The step-like disturbances with slightly smaller magnitudes than the spikes are present in the y and z components. The duration between upward and downward variations of the step-like disturbances is 80 min to 90 min,
380 not as regular as the timing for the spikes. A new type of disturbance, not evident in Fig. 1 is now clearly apparent as a variation at higher frequencies (periods less than one minute) than the steps or the spikes cadence. A closer investigation shows that this disturbance is irregular, with a maximum peak to peak amplitude of up to 4 nT in the x component and with its spectral power spread up to the Nyquist frequency.

The much smaller amplitude of the higher frequency disturbance in the y and z components indicate its linear polarization.
385 This was the disturbance which determined the orientation of the VPS used to plot the differences in Fig. 2. However, the spike-like disturbance has a large contribution on the x -component, therefore its maximum variance direction is not orthogonal to

the maximum variance direction of the high-frequency disturbance. In fact, the angle between the maximum variance directions of the spike-like disturbance and of the high-frequency disturbance is 25° , which grossly violates the orthogonality condition. As a consequence, if the two sources producing the high-frequency and the spike-like disturbances have different scaling factors, the PiCoG method will not be able to remove both disturbances from the x -component using one single pair of sensors. The 75° angle between the directions of the spike-like disturbance and the step-like disturbance is more favourable but it will still prevent the complete removal of these disturbances simultaneously unless they have the same scaling factors. The closest to orthogonality is the angle between the directions of the high-frequency disturbance and of the step-like disturbance, which is 87° . Since the orthogonality condition is not fulfilled, to proceed further we must assume that the disturbances to be removed come from a small volume compared with the distances between the sensors and therefore their scaling factors are not very different from each other. The results of the cleaning will either confirm or infirm our assumption.

For the first order correction we target the highest frequency disturbance by choosing the same window length of 100 s used to compute the VPS for the difference plotted in Fig. 2. The statistical distribution for the resulted direction (θ_w, φ_w) of the maximum variance and a histogram of the α_w values is shown in Fig. 3. Both distributions exhibit clear isolated maxima which is a strong indication that the targeted disturbance does not change its characteristics during the day interval. The angle between the disturbance directions at the two sensors is 15° , closer to collinearity than for the AMR1 correction.

Since the disturbances are larger at the inboard sensor, the effect of the correction is better illustrated for it than for the outboard sensor. The first order correction of the inboard measurements for the first four hours of the day is plotted in Fig. 4 with red over the initial AMR-corrected inboard measurements represented in the inboard VPS. The targeted high frequency disturbance is eliminated from the x component. As apparent from the top panel of Fig. 4, between 00:40 and 00:50 the high frequency disturbance was switched off. One can see that the disturber also introduces a constant offset of about 5 nT which is removed by the applied correction.

The magnitude of the spike-like disturbance is much reduced in the x component of the corrected magnetic field in Fig. 4 so we conclude that the sources of both high frequency and step-like disturbances are close to each other and are therefore removed together from the maximum variance component. This justifies the application of the PiCoG method in this particular case when the directions of the two disturbances are far from orthogonal.

For the second order correction we target the remaining spike-like disturbance by choosing a window width of 700 s. Figure 5 shows the result of the second order correction for the inboard sensor. Both the targeted spike-like disturbance and the step-like disturbance are removed from the x component by this correction step showing that indeed the distances between the sources of all three disturbances are much smaller than the distances between the disturbance sources and the FGM sensors, confirming our previous assumption.

The step-like disturbance and traces of the spike-like disturbance still remain in the y and z components in Fig. 5. To eliminate them we select a window width of 16 000 s, enough to always include at least one step-like disturbance sample. As seen in Fig. 6, the correction removes the targeted disturbance and strongly reduces the remnants of the other two disturbance types from the x component. A leftover step-like disturbance, with an magnitude of about 1 nT is still visible in the intermediate variance component. This is due to the fact that, even with carefully chosen window lengths, the maximum variance directions

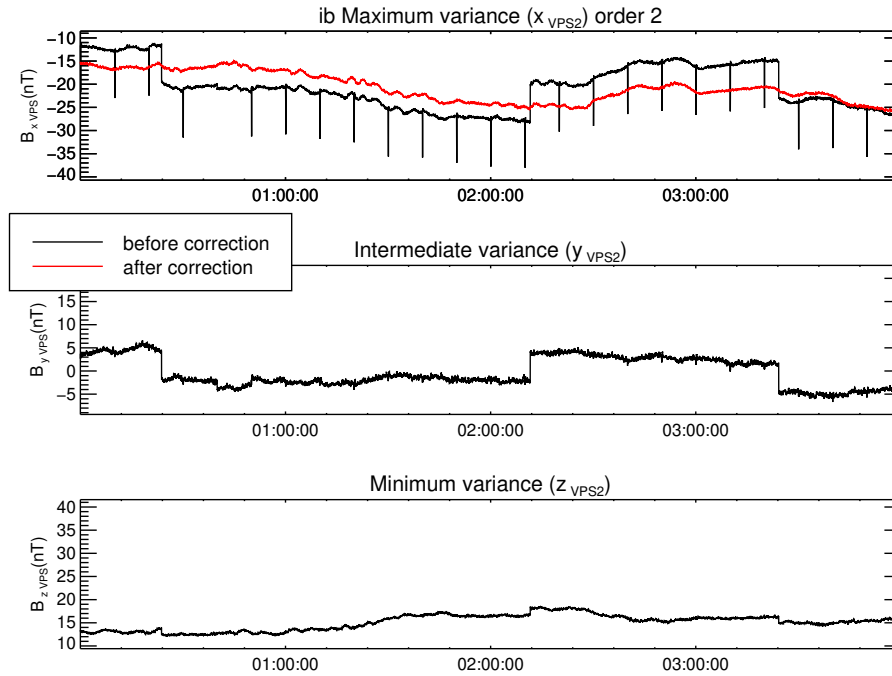


Figure 5. The first (black) and the second order correction (red) for the inboard FGM sensor. Mean values were subtracted.

are still influenced by all present disturbances, therefore do not perfectly coincide with the polarization direction of the targeted disturbances. This leads to remanent disturbance on the other components. In our case, leftovers from the high frequency disturbance interfered with the determination of the step-like disturbance polarization direction. The result is the further reduction of the high frequency disturbance at the cost of not completely removing the step-like disturbance.

We made use of the different characteristic time scales of the three disturbances treated in this section to help decouple them from one another even if their maximum variance directions were not orthogonal and even if the amplitudes of the spike-like disturbances were not much different from the amplitudes of the step-like disturbances. Would the disturbances had the same time scales, these non-ideal conditions would have prevented the PiCoG cleaning method to work, unless some other specific properties of the disturbances could have been used to help decouple them.

To check the stability of the cleaning parameters we determine them for every Sunday in 2019 with available data. The procedure produces very similar results apart from three instances when the ambient magnetic field was very disturbed. After eliminating the three outliers we computed the standard deviations for the principal component directions and for the scale factors, displayed in Table 1. The table also shows the corresponding maximum change in the corrected magnetic field on 2019.03.04 due to changes in the parameters equal to the standard deviations. The last row displays the maximum change due to the deviations in the parameters for one single order while the parameters for the other orders are kept constant. Similarly, the last column displays the maximum change related to variations either in one single direction or in one scale factor. The

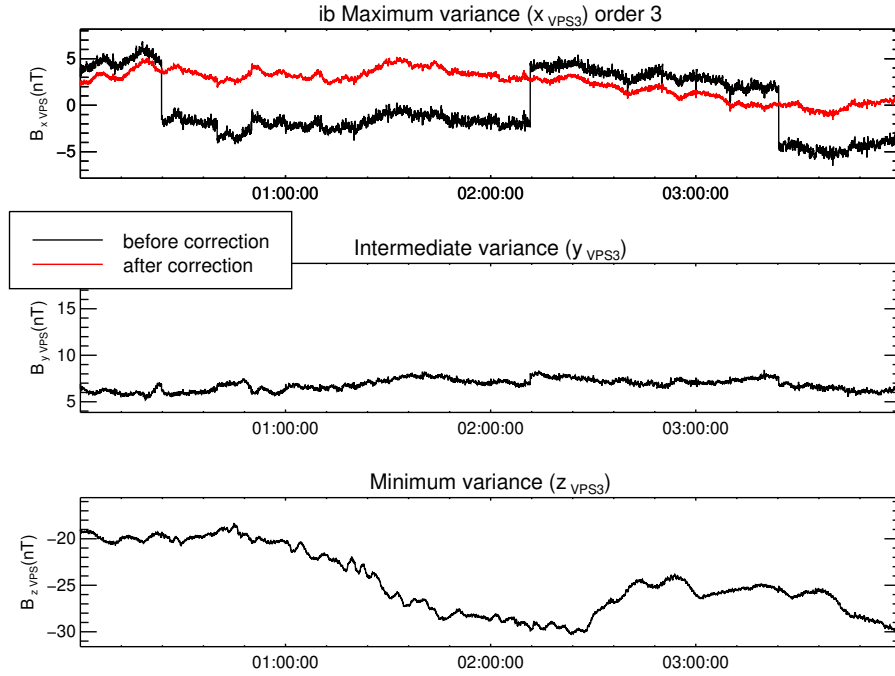


Figure 6. The second (black) and the third order correction (red) for the inboard FGM sensor. Mean values were subtracted.

last value in the table is the maximum change in the corrected magnetic field corresponding to all computed deviations, $B_{\max}^{\text{dev}} = 0.186 \text{ nT}$. This is the expected error due to the variations in the ambient magnetic field. However, the main error source
440 is related with disturbers which do not fit our assumptions such as collinearity or with the presence of higher multipoles, as discussed in section 5.

The standard deviations for the first two orders are very small, indicating very stable cleaning parameters for the high frequency disturbance and for the spike disturbance. The third order, used to clean the step-like disturbance shows larger deviations, especially for the outboard maximum variance direction. This is because of the low contribution of the step-like
445 disturbance at the outboard sensor which makes the procedure susceptible to the influence of the ambient magnetic field.

4.3 Parameters for spacecraft upload

Since the onboard correction is designed as a one-step linear combination of the measurements from different sensors, it cannot follow the iterative procedure described in section 4. Therefore, we have to write the final correction in the form:

$$B^{c,s} = \mathcal{M}^s B^{0,s} + \mathcal{M}^t B^{0,t} + \mathcal{M}^a B^{0,a} \underline{+}^s \quad (28)$$

450 where the superscript c stands for the combined correction, and the matrices \mathcal{M}^j have constant coefficients given by the \mathcal{A} correction matrices determined on ground ~~using the iterative procedure~~ from the third order correction Eq. (26) applied to the

	order 1	order 2	order 3	$\max(B_{\text{dev}})$ (nT)
direction OB (deg)	0.056	0.641	3.987	0.068
direction IB (deg)	0.066	0.265	0.625	0.105
direction ΔB (deg)	0.080	0.180	0.206	0.035
scaling factor OB	0.006	0.003	0.013	0.093
scaling factor IB	0.005	0.003	0.013	0.077
$\max(B_{\text{dev}})$ (nT)	0.064	0.082	0.114	0.186

Table 1. Standard deviations for FGMI-FGMO correction directions and scale factors, together with the corresponding maximum deviation of the corrected magnetic field.

first order AMR correction of the FGM measurements, Eq. (27):

$$\mathcal{M}^s = (\mathcal{I} + \mathcal{C}^s)(\mathcal{I} + \mathcal{A}^{0,sa}) \quad (29a)$$

$$\mathcal{M}^t = -\mathcal{C}^s(\mathcal{I} + \mathcal{A}^{0,ta}) \quad (29b)$$

$$455 \quad \mathcal{M}^a = \mathcal{C}^s \mathcal{A}^{0,ta} - (\mathcal{I} + \mathcal{C}^s) \mathcal{A}^{0,sa} \quad (29c)$$

Here \mathcal{I} denotes the identity matrix and the matrix \mathcal{C}^s has the form:

$$\begin{aligned} \mathcal{C}^s = & \mathcal{A}^{0,st} + \mathcal{A}^{1,st} + \mathcal{A}^{2,st} \\ & + \mathcal{A}^{1,st}(\mathcal{A}^{0,st} + \mathcal{A}^{0,ts}) + \mathcal{A}^{2,st}(\mathcal{A}^{0,st} + \mathcal{A}^{0,ts} + \mathcal{A}^{1,st} + \mathcal{A}^{1,ts}) \\ & + \mathcal{A}^{2,st}(\mathcal{A}^{1,st} + \mathcal{A}^{1,ts})(\mathcal{A}^{0,st} + \mathcal{A}^{0,ts}) \end{aligned} \quad (30)$$

The AC correction described in section [4.2.4](#) introduces a constant offset in the corrected data. This corresponds to the sources whose disturbances were removed. ~~In practice however~~ This DC offset can be determined by subtracting the mean value of the corrected measurements from the mean value of the original measurements:

$$460 \quad \underline{\underline{\mathbf{G}^s = \langle \mathbf{B}^{0,s} \rangle - (\mathcal{M}^s \langle \mathbf{B}^{0,s} \rangle + \mathcal{M}^t \langle \mathbf{B}^{0,t} \rangle + \mathcal{M}^a \langle \mathbf{B}^{0,a} \rangle)}} \quad (31)$$

where $\langle \dots \rangle$ denotes the average over a time interval longer than the time scale of the corrected AC disturbances.

In practice, there are additional DC offsets affecting the measurements which are treated in a separate cleaning step. The vector \mathbf{G}^s can be used to restore the original DC offset if a pure AC correction is desired.

$$465 \quad \underline{\underline{s = \mathbf{B}^{0,s} - \text{pure AC}}} \stackrel{c,s}{=} \mathcal{M}^s \mathbf{B}^{0,s} + \mathcal{M}^t \mathbf{B}^{0,t} + \mathcal{M}^a \mathbf{B}^{0,a} \pm \mathbf{G}^s \quad (32)$$

~~From equations-~~

From Eqs. (29) results that the sum of the \mathcal{M} matrices is equal to the unit matrix:

$$\mathcal{M}^s + \mathcal{M}^t + \mathcal{M}^a = \mathcal{I} \quad (33)$$

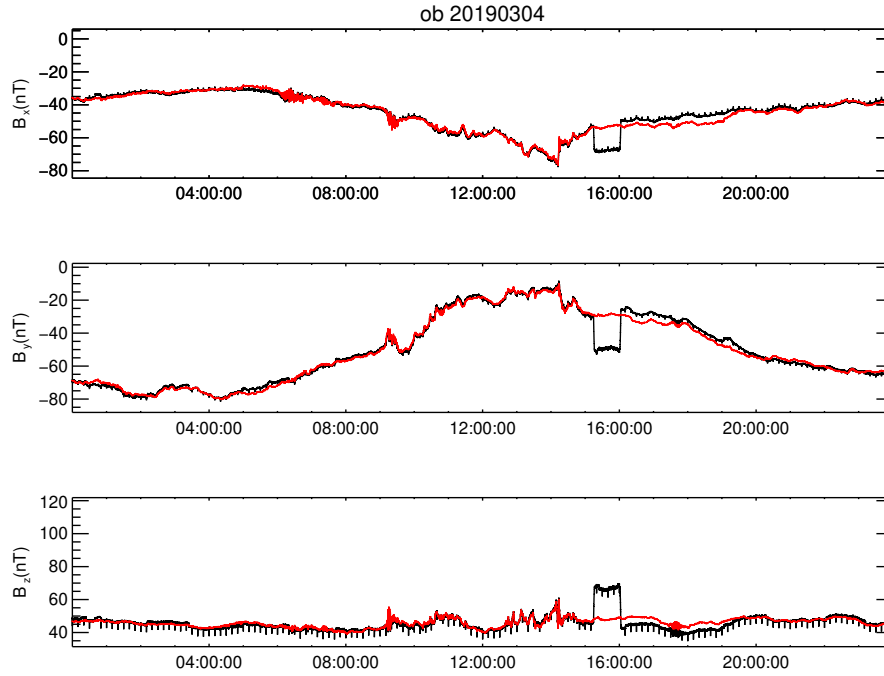


Figure 7. The final combined correction result for 2019.03.04 in the sensor system. The black lines show the original measurements taken by the outboard FGM, the red lines show the corrected data. The DC offset was restored to the value before the correction.

A consequence of Eq. (33) is that an arbitrary vector added to the measurements $B^{0,s}, B^{0,t}, B^{0,a}$ in the expression of the offset G^s in Eq. (31) vanishes, therefore G^s is independent on the ambient magnetic field. This is to be expected because the magnetic field measurements enter the correction only as differences between distinct sensors hence the correction – therefore also the offset due to the correction – is determined only by the spacecraft generated disturbances. This makes G^s a useful tool for monitoring changes in the DC offsets.

Applying Eq. (32) to the FGMO measurements yields the combined AMR1 - FGMI correction to the outboard FGM measurements. We plot the original outboard FGM measurements in sensor system with black lines and the result of the combined correction with red lines in Fig. 7.

The \mathcal{M} -matrices were uploaded on GK2A four months after its launch. Since then the magnetic field measurements are corrected onboard and transmitted to the ground stations within minutes from acquisition. The stability of the correction parameters is monitored and a new set of parameters will be computed and uploaded in case changes in the spacecraft operation will require a change in the parameters.

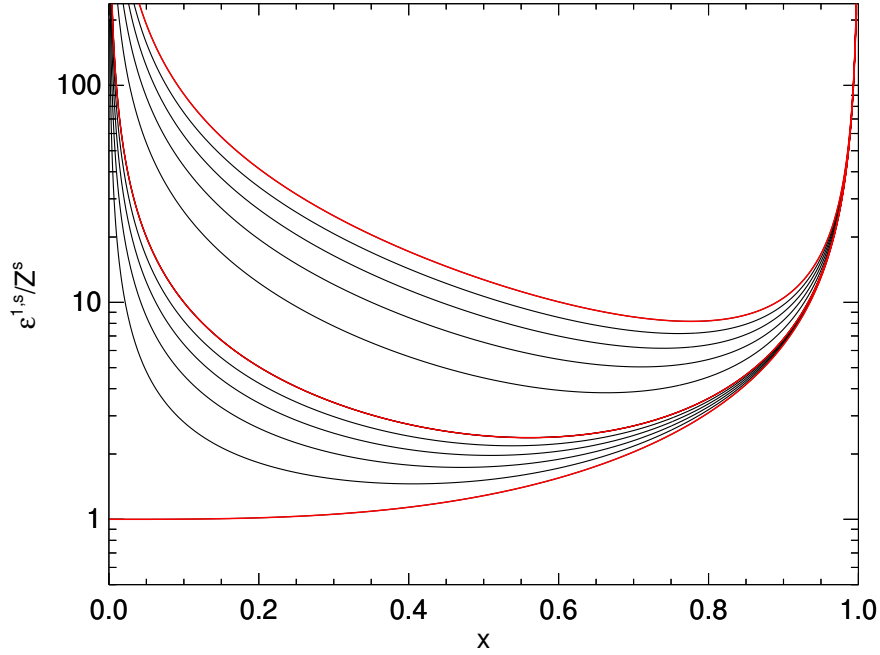


Figure 8. The error due to sensor specific disturbances and to the quadrupole disturbance introduced by PiCoG dipole disturbance correction. The x -axis represents the position $x = r^t/r^s$ of the inboard sensor relative to the outboard sensor. Sensor noise is the same for both sensors. Each line corresponds to a fixed value of the quadrupole disturbance at the outboard position. Red lines, bottom to top: $b_q^s = (0, 1 \text{ and } 10) \times Z^s$. The black lines in between correspond to $(0.2, 0.4, 0.6 \text{ and } 0.8) \times Z^s$ and $(2, 4, 6 \text{ and } 8) \times Z^s$, respectively.

5 Errors and limitations

Even though we were able to eliminate most of the magnetic field disturbances onboard the GK2A spacecraft, we need to be aware of the limitations the proposed method is subject to. We have already seen that due to other disturbances or due to the ambient magnetic field variations, the maximum variance direction might not coincide with the polarization direction of the disturbance to be removed. This ~~slight~~ difference will cause non-zero projections of the disturbance on the intermediate and minimum variance direction components which are not removed by the current applied correction. They will be reduced however by the next correction if the targeted sources lie close to each other. A disturbed ambient magnetic field may also interfere with the determination of the scaling factors. While there are ways to mitigate these effects, they are not within the scope of the present work.

490 An important benefit of the PiCoG method is the ability to treat up to three separate disturbance sources using measurements from two sensors. In order to be able to decouple the individual disturber contributions, two conditions must be satisfied: the disturbances must have well defined polarization directions and these directions must be orthogonal to each other. This may

seem a strong condition to impose. However, apart from moving mechanisms such as reaction wheels, many, if not most of the magnetic disturbances from a spacecraft come from current loops without phase delays and are therefore linearly polarized. The orthogonality on the other hand, is not guaranteed. Even in the non-orthogonal case, disturbances coming from sources close to each other compared to the distance to the sensors share the same scaling factor (if both are either dipoles or quadrupoles) and are therefore removed together. A possible way to treat non-orthogonal disturbances coming from positions separated by large distances compared to the distances to the sensors is first transforming the data to a non-orthogonal system with its axes aligned with the maximum variance directions of the three largest disturbers. This exercise is left for future examination.

Another For each correction order, the disturbance to be removed has to be decoupled from the other disturbances. This is the case if the targeted disturbance amplitude is much larger than the amplitudes of the other disturbances, as assumed in section 3.1. Another situation when the disturbances can be decoupled is when they have different characteristic time scales. Then one may either use windowing in the time domain, as done in section 4.2, or use a band-pass filtering in frequency domain. If the disturbances cannot be decoupled, then the cleaning procedure only works if the distances between the disturbance sources which cannot be separated are small compared to the distances to the sensors used for cleaning. In this case the cleaning parameters are similar, and the coupled disturbances are cleaned together.

One important class of error sources are additional disturbances which do not follow the determined scaling factor α or that are present at one sensor only. Among these are the sensor specific noise, temperature effects which sometimes cause sensor offset oscillations, and multipoles of higher order than the targeted disturbance. These disturbances are introduced into the cleaned magnetic field data either reduced or enhanced, depending on the sensor positions. In particular for GK2A, sensor offset oscillations triggered by large temperature gradients are quite significant reaching peak to peak amplitudes up to 5 nT in the cleaned data (Magnes et al., 2020).

To estimate the error introduced by the sensor specific noise combined with a quadrupole contribution additional to a dipole disturbance to be removed, let us assume a simple collinear geometry: A disturber placed in the origin of the coordinate system producing a disturbance characterized by both a dipole moment \mathbf{M} and a quadrupole moment \mathbf{Q} , an inboard sensor placed at the distance r^t characterized by a sensor specific noise \mathbf{Z}^t , and an outboard sensor placed at the distance r^s characterized by a sensor specific noise \mathbf{Z}^s . In these conditions, the correction of the dipole disturbance will introduce an error stemming from the quadrupole disturbance and the sensor specific disturbances. The magnitude of the error will depend on the relative positions of the two sensors, on the sensor specific noise and on the strength of the quadrupole disturbance. After projecting on the principal component direction, the magnetic field measured by the outboard sensor is (dropping the x component index):

$$B^{0,s} = B + b_d^s + b_q^s + Z^s \quad (34)$$

where b_d^s and b_q^s represent the disturbance dipole and quadrupole contributions at the outboard sensor. A similar expression can be written for the inboard sensor.

The corrected field is obtained by applying equation (13a):

$$B^{1,s} = B + \epsilon^{1,s} \quad (35)$$

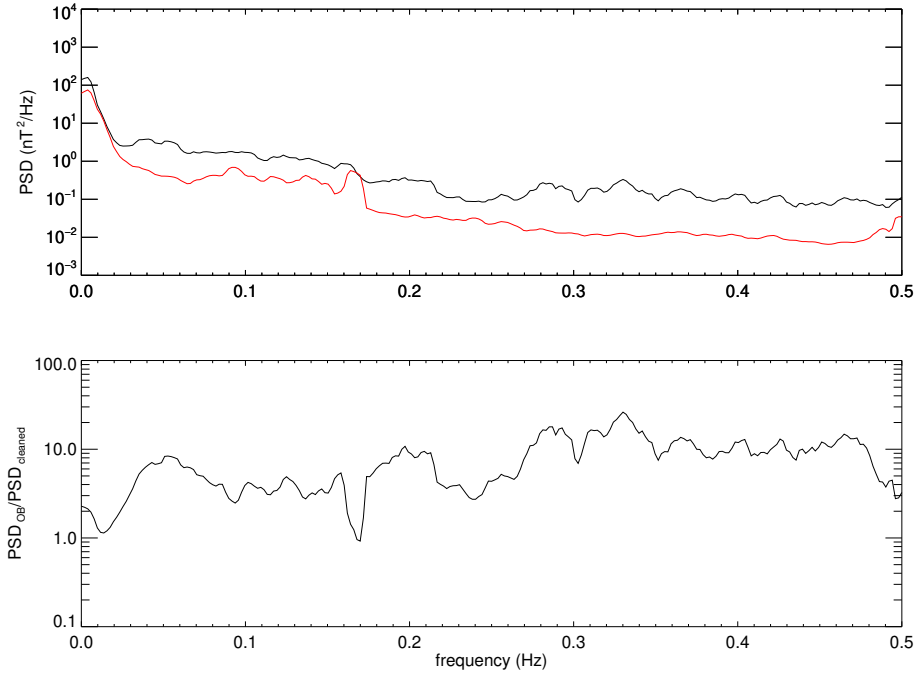


Figure 9. Top panel: Power spectral density of the initial FGMO measurements (black line) compared with the PSD of the cleaned data (red line). Bottom panel: the ratio between the initial and cleaned PSDs for 2019.03.04.

with the error $\epsilon^{1,s}$ given by

$$\epsilon^{1,s} = (1 - \alpha)Z^s + \alpha Z^t + (1 - \alpha)b_q^s + \alpha b_q^t \quad (36)$$

Making the notation

$$x = \frac{r^t}{r^s} < 1 \quad (37)$$

530 and keeping in mind that $b_d^s = x^3 b_d^t$ and $b_q^s = x^4 b_q^t$, equation (36) becomes:

$$\epsilon^{1,s} = \frac{1}{1 - x^3} \left[1 + x^3 \frac{Z^t}{Z^s} + \left(\frac{1}{x} - 1 \right) \frac{b_q^s}{Z^s} \right] Z^s \quad (38)$$

Similar with Neubauer (1975) findings, the optimum position x results from a trade off between the error due to the sensors, Z , and the error due to higher order multipoles, b_q . We plot the error given by equation (38) for a number of quadrupole strengths in Fig. 8. The bottom red line corresponds to zero quadrupole moment. In this case, minimum error, equal to the
535 outboard sensor specific noise, is obtained for $x = 0$, i.e. for the inboard sensor placed at the position of the dipole disturber. As soon as a higher multipole is present, the inboard sensor must be moved away from the disturbance source in order to minimize the error. Already for a quadrupole disturbance at the outboard position equal to a tenths of the sensor noise, the

optimum position of the inboard sensor is almost at the mid distance between the disturber and the outboard sensor. When the quadrupole disturbance becomes equal with the sensor noise, the optimum distance becomes about $0.6x$ (mid red line). If the boom is very short, the quadrupole disturbance at the outboard sensor can reach very large values. The topmost red line in Fig. 8 corresponds to a quadrupole contribution ten times as large as the outboard sensor noise. In this case the optimum position of the inboard sensor approaches even more the outboard sensor position ($0.8x$).

A way to estimate the overall performance of the cleaning is to compare the power spectral densities of the initial measurements with the PSDs of the cleaned data as shown in Fig. 9. The spectra in the figure were computed as the average over the entire 2019.03.04 day using a sliding window of 512 s. Both PSDs contain not only the (remaining) disturbances but also the ambient magnetic field. Their difference shows the absolute total power of the removed disturbances, while their ratio represents the minimum factor with which the power of the disturbances is reduced. The mean of this factor for the 24 h interval shown in Fig. 9 over the frequency range covering periods from 2 s to 1 min is equal to 7.8. For lower frequencies, in the range covering periods between 1 min to 6 h we obtain a factor of 3.9 from the PSDs computed without windowing.

The success of the cleaning procedure can also be estimated for each individual disturbance class. The initial magnitudes of the disturbances targeted for cleaning are shown in Table 2 for each sensor. Values are given for each component in the OSRF and for the module. The last column shows the remnants of the disturbances in the corrected data.

For the midnight disturbance we separated the leading ramp occurring around 15:00 UT from the abrupt trailing ramp about one hour later. The magnitude is computed as the difference between the median over 1.5 min of the field before and after the ramp. The leading ramp is reduced from about 34 nT in the FGMO measurements to less than 2 nT in the corrected measurements. The trailing ramp is reduced from 40 nT to about 1 nT. For the components, positive sign denotes upward ramp and negative sign downward ramp.

The ramps of the step-like disturbances are symmetric therefore we do not differentiate between the leading and the trailing ramps. The magnitudes are computed in the same way as for the MD. The mean step magnitude is reduced from 2.5 nT to 1.3 nT. However, note that the x component is more than doubled, from 0.4 nT to 1 nT. This is a necessary compromise we have to make because the polarization directions of the disturbances are not orthogonal, as discussed in sec. 4.2.

The magnitude for the spikes was computed as the difference between the value of the peak of the spike and the median over 20 s intervals 5 s before and 5 s after the peak of the spike. For 2019.03.04 we obtain a mean magnitude of 13.8 nT for the initial FGMI measurements, 4.9 nT for the FGMO initial measurements, and 0.3 nT for the corrected measurements. For the components, positive sign denotes upward spikes and negative sign downward spikes.

To estimate the reduction of the high frequency disturbance we use as disturbance-free etalon the quiet 10 min interval visible in Fig. 4 between 00:40 and 00:50. The magnitude of the high frequency disturbance is computed as the difference between the mean peak to peak amplitude ($2\sqrt{2\langle B^2 \rangle_{\text{time}}}$) of the measurements during the reference quiet interval – which is 0.2 nT for the corrected measurements – and the mean peak to peak amplitude over the adjacent interval between the next two spikes. The result is below 0.1 nT for all components and for the module. Note that while AMR1 does not detect a quiet interval, it is still affected by a disturbance in the high frequency range of about 18 nT peak to peak amplitude, possibly coming from another source(s). Despite the large amplitude of this disturbance at AMR1, the increase of the disturbance in the high frequency range

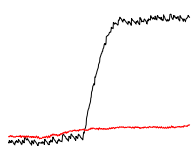
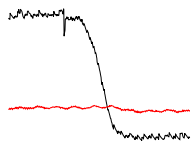
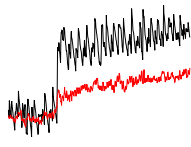
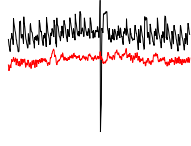
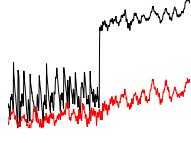
disturbance class	component	AMR 1	AMR 2	FGMI	FGMO	corrected
magnitude (nT)						
	x	-612.0	-117.8	-36.7	-15.1	-0.1
	y	-1352.8	-7.2	-28.1	-20.2	-0.6
	z	467.3	166.8	35.7	22.2	1.7
	module	1556.6	204.3	58.4	33.6	1.8
	x	764.5	145.2	45.1	17.6	-0.8
	y	1684.0	10.8	35.1	24.7	0.2
	z	-548.7	-203.8	-42.9	-26.0	-0.8
	module	1929.1	250.5	71.5	40.0	1.1
	x	5.8	24.0	4.6	0.4	1.0
	y	3.3	13.5	2.6	1.7	0.6
	z	3.9	22.2	8.7	1.9	0.7
	module	7.7	35.4	10.2	2.5	1.3
	x	4.3	-6.4	-5.4	0.6	-0.2
	y	2.2	-2.0	-4.7	-1.8	-0.2
	z	1.9	-4.1	-11.8	-4.6	-0.1
	module	5.2	7.9	13.8	4.9	0.3
	x		0.7	1.4	0.4	0.1
	y		0.1	1.1	0.3	0.0
	z		0.3	1.5	0.7	0.1
	module		0.8	2.3	0.9	0.1

Table 2. The initial magnitudes of the disturbances at all sensors and the final magnitudes in the corrected data for 2019.03.04. For the MD and for the spikes the sign shows the direction of the disturbance. AMR1 does not detect a quiet interval therefore we cannot estimate the HF disturbance magnitude at AMR1. The MD and the steps magnitudes are defined as the size of their ramps. The magnitudes of the spikes are equal with the spikes heights/depths. The high frequency disturbance magnitude is defined as the peak to peak amplitude. Samples of the disturbances affecting the z component of the outboard sensor (black lines), together with the corrected measurements (red lines) over ten minute intervals are illustrated in the second column.

of the FGMO and FGMI measurements after the AMR correction is below 0.1 nT. All other discussed disturbances apart from the MD are lower at AMR1, which combined with the large scale factor used for correcting the MD assures minimum transfer of these disturbances to the corrected data.

6 Summary and conclusions

We propose a multi-sensor method for removing spacecraft generated AC disturbances from magnetic field data. The method employs principal component analysis to decouple multiple disturbance sources and minimize the introduction of artefacts to the components free of the targeted disturbance.

580 A pair of sensors can resolve up to three independent disturbers. While no prior knowledge on the disturber source is required, linear polarization of the disturbance is assumed, and the polarization direction of different disturbers should ideally be mutually orthogonal. The method is robust enough to provide sensible results even if these assumptions are not strictly met. Of course, specific situations may provide additional opportunities to help separating distinct disturbers. One example is using the different characteristic time scales of the disturbances to determine the window lengths in section 4.

585 There are however situations, such as non orthogonal disturbances from sources with large spatial separation compared with the distance to the sensors when two sensors are not enough to remove the disturbances with the described ~~algorithm~~method. Not linearly polarized disturbances, as those produced by reaction wheels, need special treatment not covered by this work.

We applied the PiCoG cleaning method to the GK2A SOSMAG sensor configuration by first using the spacecraft-body mounted AMR sensor measurements to remove large disturbances from the two boom mounted FGM sensors. Three distinct types of disturbances were then removed using the two FGM sensor measurements: high frequency disturbance in less than 1 min range, spikes occurring every 10 min, and steps occurring at intervals above 1 h.

We proved that on a specific day the method was able to reduce the spectral power of magnetic field disturbances by at least a factor of 7.8 in the period range of 2 s to 1 min and 3.9 in the period range of 1 min to 6 h. These values are representative for the performance of the method over the entire 2019 year.

595 The final correction takes the form of a linear combination of the different sensor readings whose coefficients were determined on ground. These coefficients were uploaded to the GK2A spacecraft, allowing for in-flight removal of spacecraft disturbances and near real-time delivery of cleaned magnetic field data, essential for space-weather applications. In future we shall apply the PiCoG method for post-processing of data from other spacecraft, e.g. from BepiColombo (Benkhoff et al., 2010) and Cluster.

600 *Data availability.* SOSMAG data can be requested from the European Space Agency (ESA) and from the National Meteorological Satellite Center (NMSC) of the Korea Meteorological Administration (KMA)

Author contributions. All authors contributed equally to the manuscript.

Competing interests. The authors declare that they have no conflict of interest.

Acknowledgements. This work was financially supported by the Deutsches Zentrum für Luft- und Raumfahrt under contracts 50OC1803 and
605 50OC1403, by the General Support Technology Programme of ESA, contract 4000105630, and by the Space Situational Awareness (SSA)
Programme of ESA, contract 4000117456.

References

- Acuña, M. H.: Space-based magnetometers, *Review of Scientific Instruments*, 73, 3717–3736, <https://doi.org/10.1063/1.1510570>, 2002.
- Angelopoulos, V.: The THEMIS mission, *Space Sci. Rev.*, pp. 47–+, <https://doi.org/10.1007/s11214-008-9336-1>, 2008.
- 610 Auster, H. U., Glassmeier, K. H., Magnes, W., Aydogar, O., Constantinescu, O. D., Fischer, D., Fornaçon, K. H., Georgescu, E., Harvey, P., Hillenmaier, O., Kroth, R., Ludlam, M., Narita, Y., Okrafka, K., Plaschke, F., Richter, I., Schwarzl, H., Stoll, B., Valavanoglu, A., and Wiedemann, M.: The THEMIS fluxgate magnetometer, *Space Sci. Rev.*, pp. 73–+, <https://doi.org/10.1007/s11214-008-9365-9>, <http://www.springerlink.com/content/fr4u42m531431m34/>, 2008.
- Auster, U., Magnes, W., Delva, M., Valavanoglou, A., Leitner, S., Hillenmaier, O., Strauch, C., Brown, P., Whiteside, B., Bendyk, M.,
615 Hilgers, A., Kraft, S., Luntama, J. P., and Seon, J.: Space Weather Magnetometer Set with Automated AC Spacecraft Field Correction for GEO-KOMPSAT-2A, in: *ESA Workshop on Aerospace EMS*, vol. 738 of *ESA Special Publication*, p. 37, 2016.
- Balogh, A.: Planetary Magnetic Field Measurements: Missions and Instrumentation, *Space Sci. Rev.*, 152, 23–97, <https://doi.org/10.1007/s11214-010-9643-1>, 2010.
- Behannon, K. W., Acuna, M. H., Burlaga, L. F., Lepping, R. P., Ness, N. F., and Neubauer, F. M.: Magnetic Field Experiment for Voyagers
620 1 and 2, *Space Sci. Rev.*, 21, 235–257, <https://doi.org/10.1007/BF00211541>, 1977.
- Benkhoff, J., van Casteren, J., Hayakawa, H., Fujimoto, M., Laakso, H., Novara, M., Ferri, P., Middleton, H. R., and Ziethe, R.: BepiColombo—Comprehensive exploration of Mercury: Mission overview and science goals, *Planet. Space Sci.*, 58, 2–20, <https://doi.org/10.1016/j.pss.2009.09.020>, 2010.
- Brown, P., Beek, T., Carr, C., O’Brien, H., Cupido, E., Oddy, T., and Horbury, T. S.: Magnetoresistive magnetometer for space science
625 applications, *Measurement Science and Technology*, 23, 025902, <https://doi.org/10.1088/0957-0233/23/2/025902>, 2012.
- Delva, M., Feldhofer, H., Schwingenschuh, K., and Mehlem, K.: A new multiple sensor magnetic compatibility technique for magnetic field measurements in space, in: *International Symposium on Electromagnetic Compatibility*, edited by ed Elettronica Italiana, A. E., EMC Europe, pp. 523–528, 2002.
- Dougherty, M. K., Kellock, S., Southwood, D. J., Balogh, A., Smith, E. J., Tsurutani, B. T., Gerlach, B., Glassmeier, K. H., Gleim, F.,
630 Russell, C. T., Erdos, G., Neubauer, F. M., and Cowley, S. W. H.: The Cassini Magnetic Field Investigation, *Space Sci. Rev.*, 114, 331–383, <https://doi.org/10.1007/s11214-004-1432-2>, 2004.
- Escoubet, C. P., Schmidt, R., and Goldstein, M. L.: Cluster: Science and Mission Overview, *Space Sci. Rev.*, 79, 11–32, 1997.
- Georgescu, E., Auster, H. U., Takada, T., Gloag, J., Eichelberger, H., Fornaçon, K. H., Brown, P., Carr, C. M., and Zhang, T. L.: Modified gradiometer technique applied to Double Star (TC-1), *Advances in Space Research*, 41, 1579–1584, <https://doi.org/10.1016/j.asr.2008.01.014>,
635 2008.
- Herčík, D., Auster, H.-U., Blum, J., Fornaçon, K.-H., Fujimoto, M., Gebauer, K., Güttler, C., Hillenmaier, O., Hördt, A., Liebert, E., Matsuoka, A., Nomura, R., Richter, I., Stoll, B., Weiss, B. P., and Glassmeier, K.-H.: The MASCOT Magnetometer, *Space Sci. Rev.*, 208, 433–449, <https://doi.org/10.1007/s11214-016-0236-5>, 2017.
- Kato, M., Sasaki, S., and Takizawa, Y.: The Kaguya Mission Overview, *Space Sci. Rev.*, 154, 3–19, <https://doi.org/10.1007/s11214-010-9678-3>, 2010.
640
- Magnes, W., Hillenmaier, O., Auster, U., Brown, P., Kraft, S., Seon, J., Delva, M., Valavanoglou, A., Leitner, S., Fischer, D., Narita, Y., Wilfinger, J., Strauch, C., Ludwig, J., Constantinescu, D., Fornaçon, K.-H., Gebauer, K., Herčík, D., Richter, I., Eastwood, J., Luntama,

- J., Na, G.-W., Lee, C.-H., and Hilgers, A.: SOSMAG: Space Weather Magnetometer aboard GEO-KOMPSAT-2A, *Space Sci. Rev.*, in preparation, 2020.
- 645 Mehlem, K.: Multiple magnetic dipole modeling and field prediction of satellites, *IEEE Transactions on Magnetism*, 14, 1064–1071, <https://doi.org/10.1109/TMAG.1978.1059983>, 1978.
- Narvaez, P.: The Magnetostatic Cleanliness Program for the Cassini Spacecraft, *Space Sci. Rev.*, 114, 385–394, <https://doi.org/10.1007/s11214-004-1433-1>, 2004.
- Ness, N. F., Behannon, K. W., Lepping, R. P., and Schatten, K. H.: Use of two magnetometers for magnetic field measurements on a spacecraft, *J. Geophys. Res.*, 76, 3564, <https://doi.org/10.1029/JA076i016p03564>, 1971.
- 650 Ness, N. F., Behannon, K. W., Lepping, R. P., Whang, Y. C., and Schatten, K. H.: Magnetic Field Observations near Venus: Preliminary Results from Mariner 10, *Science*, 183, 1301–1306, <https://doi.org/10.1126/science.183.4131.1301>, 1974.
- Neubauer, F. M.: Optimization of multimagnetometer systems on a spacecraft, *J. Geophys. Res.*, 80, 3235, <https://doi.org/10.1029/JA080i022p03235>, 1975.
- 655 Oh, D., Kim, J., Lee, H., and Jang, K.-I.: Satellite-based In-situ Monitoring of Space Weather: KSEM Mission and Data Application, *Journal of Astronomy and Space Sciences*, 35, 175–183, <https://doi.org/10.5140/JASS.2018.35.3.175>, 2018.
- Pope, S. A., Zhang, T. L., Balikhin, M. A., Delva, M., Hvizdos, L., Kudela, K., and Dimmock, A. P.: Exploring planetary magnetic environments using magnetically unclean spacecraft: a systems approach to VEX MAG data analysis, *Ann. Geophys.*, 29, 639–647, <https://doi.org/10.5194/angeo-29-639-2011>, 2011.
- 660 Primdahl, F.: The fluxgate magnetometer, *Journal of Physics E: Scientific Instruments*, 12, 241–253, 1979.
- Seon, J., Chae, K. S., Na, G. W., Seo, H. K., Shin, Y. C., Woo, J., Lee, C. H., Seol, W. H., Lee, C. A., Pak, S., Lee, H., Shin, S. H., Larson, D. E., Hatch, K., Parks, G. K., Sample, J., McCarthy, M., Tindall, C., Jeon, Y. J., Choi, J. K., and Park, J. Y.: Particle Detector (PD) Experiment of the Korea Space Environment Monitor (KSEM) Aboard Geostationary Satellite GK2A, *Space Sci. Rev.*, 216, 13, <https://doi.org/10.1007/s11214-020-0636-4>, 2020.
- 665 Song, P. and Russell, C. T.: Time Series Data Analyses in Space Physics, *Space Sci. Rev.*, 87, 387–463, <https://doi.org/10.1023/A:1005035800454>, 1999.
- Sonnerup, B. U. Ö. and Scheible, M.: Minimum and Maximum Variance Analysis, in: *Analysis methods for multi-spacecraft data*, edited by Paschmann, G. and Daly, P., ISSI Sci. Rep. SR-001, pp. 185–220, ISSI, Bern, 1998.
- Titov, D. V., Svedhem, H., McCoy, D., Lebreton, J. P., Barabash, S., Bertaux, J. L., Drossart, P., Formisano, V., Haeusler, B., Korabely, O. I., Markiewicz, W., Neveance, D., Petzold, M., Piccioni, G., Zhang, T. L., Taylor, F. W., Lellouch, E., Koschny, D., Witasse, O., Warhaut, M., Acomazzo, A., Rodrigues-Cannabal, J., Fabrega, J., Schirmann, T., Clochet, A., and Coradini, M.: Venus Express: Scientific goals, instrumentation, and scenario of the mission, *Cosmic Research*, 44, 334–348, <https://doi.org/10.1134/S0010952506040071>, 2006.
- 670 Zhang, T. L., Baumjohann, W., Delva, M., Auster, H. U., Balogh, A., Russell, C. T., Barabash, S., Balikhin, M., Berghofer, G., Biernat, H. K., Lammer, H., Lichtenegger, H., Magnes, W., Nakamura, R., Penz, T., Schwingenschuh, K., Vörös, Z., Zambelli, W., Fornacon, K. H., Glassmeier, K. H., Richter, I., Carr, C., Kudela, K., Shi, J. K., Zhao, H., Motschmann, U., and Lebreton, J. P.: Magnetic field investigation of the Venus plasma environment: Expected new results from Venus Express, *Planet. Space Sci.*, 54, 1336–1343, <https://doi.org/10.1016/j.pss.2006.04.018>, 2006.